Markov Chain Modelling for Time Evolution of Internal Pitting Corrosion Distribution of Oil and Gas Pipelines

Chinedu I. Ossai, Brian Boswell and Ian Davies

(Department of Mechanical Engineering, Curtin University, GPO Box U1987, Perth, WA 6845, Australia)

Abstract

A continuous time non-homogenous linear growth pure birth Markov model was used to predict the future pit depth distribution of internally corroded oil and gas pipelines. A negative binomial distribution was used for calculating the transition probability functions of the pit depths whilst pit depths growth was estimated for low, moderate, high and severe pitting corrosion rates using field measured data of pit depths, temperatures, CO_2 partial pressures, pH and flow rates. The Markov predicted results agreed well with field measured pit depth data from X52 grade pipeline and L-80 and N-80 grades offshore well tubing.

Keywords: A. Mild steel; B. Modelling studies; C. Pitting Corrosion

1.0 Introduction

Pitting process can be metastable in nature - a situation in which a pitting process starts and stops after a while or immediately [1, 2] or it can be a stable pitting that nucleates and grows indefinitely. Stable pits generally show stochastic behaviour [1, 3] and are the focus of many researches. Pitting corrosion is initiated due to:

i. Electrochemical reactions of the carbon steel surfaces with the environment resulting in formation of surface layers.
ii. Discontinuity of the carbon steel material as a result of inclusions.
iii. Removal of already formed surface layer due to erosion [4].

Forecasting of pitting corrosion rate has been done by modelling, extrapolation or using expert judgement [5]. Modelling technique can follow either probabilistic, deterministic or both approaches and has widespread application as exemplified by numerous publications [1, 6-7, 8, 9]. Yusof *et al.* [6] studied pitting corrosion of offshore pipelines with Markov chain model and discovered that the prediction was not conservative due to the assumption that the model is linear. The data for the analysis was from repeated in-line inspection (ILI) of internal corroded offshore pipelines.

Corresponding author: Chinedu I. Ossai
Tel : +61404581441
Email address: ossaic@gmail.com

The authors assumed time of initiation of internal pitting corrosion as 2.9 years (after Velazquez *et al.* (10)) which is time of initiation of underground pipeline external pitting corrosion. This assumption may invalidate the result of these authors since the environmental condition of the soil is definitely different from that inside the pipeline. Although the future predicted pit depth distribution in this work was based on the exponential parameter (V_p) of power law being 1, the authors proposed Equation (1) for predicting the value of V for future pit depth distribution if the initial pit depth (P_{d_1}) and time (t_1) and future pit depth (P_{d_2}) and time (t_2) are known with the pitting initiation time (t_{int}).

$$V_p = \frac{log\left(\frac{P_{d_2}}{P_{d_1}}\right)}{log\left(\frac{t_2 - t_{int}}{t_1 - t_{int}}\right)} \quad (1)$$

The work of Valor *et al.* [1] focused on pitting corrosion of underground pipelines and corrosion coupons. The authors used discrete pit depths in non-homogenous, continuous time Markov chain modelling to determine the transition probability function by correlating the stochastic mean pit depth with the empirical deterministic pit depth. They used Weibull process for simulation of the pitting induction time. Other researchers such as Bolanos-Rodriguez *et al.* [11], Valor *et al.* [12] and Rodriguez III *et al.* [13] also applied non-homogenous, continuous time pure birth Markov chain modelling to estimate the pit depth distribution of pipelines by using a closed form of Kolmogorov forward equation for computation of the transition probability function whilst assuming that the pit depth follows a stochastic process. Similarly, Camacho *et al.* [14] applied Fokker-Planck equation for transition probability function estimate of pitting corrosion of underground pipelines based on a continuous time, non-homogenous pit depth evolution and Hong [15] worked on pit initiation and growth processes by modelling pit initiation as a homogenous Poisson process whilst estimating the pit growth with time as a non-homogenous, continuous time Markov process.

Pipeline failures resulting from pitting have been attributed to pin-hole type pit [8] hence, the need for extreme value modelling of maximum pit depths of corroded pipelines to predict the distribution in the future. Valor *et al.* [8] applied a stochastic modelling approach to estimate the extreme value distribution of corroded low carbon steel using API-5L X52 pipeline corrosion coupons experimental data. Melchers [16] showed that extreme value analysis can be carried out with limited data if it is combined with Bayesian approach and demonstrated this feat with carbon steel coupons exposed to marine environment. Similarly, Melchers [17] used a bi-modal probability density function to represent the maximum pit depth distribution of mild steel exposed to marine environment and concluded that maximum pit depth distribution is better

represented with Fretchet distribution for a long-time exposure of the material than Gumbel distribution that is traditionally used for the extreme value distribution plotting [1-3, 5, 18-19] however, Sheikh *et al.* [9] showed that the initial pitting corrosion followed a normal distribution and lognormal distribution for long-time exposure of carbon steel material to a corrosive environment.

Sulphate Reducing Bacteria (SRB) are the most active contributor to pitting in long-time exposure of carbon steel materials to marine environment [2] because their metabolic activities results in sulphate ion reduction to hydrogen and sulphide. The sulphide ion attacks the steel electrochemically causing more pitting corrosion due to an increase in anodic/cathodic reactions necessitated by sulphate reduction. Other researchers also found out experimentally that sulphur reducing bacteria starved of organic energy sources cause severe pitting corrosion of carbon steel materials [20]. Although cathodic protection and other forms of coating have the ability of protecting marine infrastructures like pipelines from external pitting corrosion, ageing infrastructures exposed to marine environment have serious problem of pitting corrosion which can predominantly cause assets failures. Rivas *et al.* [3] used block maxima and peak over threshold approach for extreme value analysis of laboratory simulated field data of buried carbon steel pipeline and concluded that the peak over threshold approach was more robust in estimating the maximum pit depth of the samples. In their own work, Valor *et al.* [21] described pit initiation and propagation as a stochastic process of non-homogenous Poisson process and non-homogenous continuous time Markov process respectively. They used extreme value statistics for modelling maximum pit growth for data obtained from literature. Although the work produced better results than those obtained from available literature (see ref [21]), however, the assumption that the entire pits tested nucleates instantaneously may not always be the case practically.

Corrosion can result in unscheduled downtime especially for pitting corrosion, crevice corrosion, stress corrosion cracking and fatigue corrosion since they occur without outward signs on the facilities [22]. Hence, corrosion modelling is used for integrity management via prediction of expected time of pipeline failure so that mitigation actions that could include inspection and repairs will be initiated [7-8, 23-24]. To establish the time dependent reliability of corroded high pressure offshore pipelines, Zhang and Zhou [25] determined the expected future internal corrosion wastage distribution due to internal pressure using Poisson square wave process. The authors established the time of pipeline failure with respect to small leak, large leak and rupture by using in-line inspection data after modelling stochastic pit depth growth with homogenous gamma distribution according to Equation (2):

$$f_G(P_d(t)|\alpha(t-t_{int}),\beta) = \frac{\beta^{\alpha}(t-t_{int}) * P_d(t)^{\alpha(t-t_0)-1} * e^{-P_d(t)^{\beta}} * I(t)}{\Gamma(\alpha(t-t_{int}))} \quad (2)$$

where $f_G(P_d(t)|\alpha(t-t_0),\beta)$ is the probability density function of the pit depth at time t, $\alpha(t-t_0)$ is the time dependent shape parameter, $\Gamma(.)$ is the gamma function, $I(t)$ is an indicator function with values given in Equation (3).

$$I(t)=\begin{cases}1 & if \quad t > t_{int}\\ 0 & if \;\; 0 \le t \le t_{int}\end{cases} \tag{3}$$

Bazán and Beck [26] also used Poisson square wave process to model external pitting corrosion of underground pipelines and concluded that power model gave a more conservative estimate of the future corrosion wastage than random linear model after comparing the results with field inspection data. Similarly, Valor *et al.* [27] used historic data to determine the reliability of corroded non-piggable upstream pipelines exposed to external corrosion by statistically analysing the acquired data, determining the corrosion distribution at a future time and correlating the results with the designed pipeline failure pressure. The aim of these researchers is to establish a mitigation program aimed at enhancing the lifecycle of the pipelines [27]. The work of Rodriguez III *et al.* [28] was also aimed at mitigation and control of pitting corrosion by applying Markov chain modelling to determine the future pit depth whilst predicting the remaining useful life of the pipeline at future times based on the pit depth distribution.

Other pitting corrosion related researches that are noteworthy includes the work of Valor *et al.* [23] that used Monte Carlo reliability framework to model different corrosion distributions that included linear growth model, time dependent and time independent models ,Markov model and single value distribution model. They utilized both synthetic and field data in evaluating these models whilst considering defect sizes, age and depth of corrosion with time. They concluded that Markov chain predictive model was best for describing the corrosion distributions [23]. Caleyo *et al.* [19] also used Monte Carlo simulation to model pit depth growth of underground pipelines in different soil conditions and fitted the three maximal extreme value distributions - Weibull, Fretchet and Gumbel to the resulting best fit models of the studied soils, however, Fretchet distribution was best for describing the best fit model over a long-time exposure as was already stated in this work. Again, another work on experimental determination of internal pitting rate in pipelines concluded that increases in pitting rate occurs due to increased chloride concentration, temperature, subcutaneous substances (such as sand) and flow rate whereas decrease in pitting rate was observed with increase in bicarbonate, CO_2 and H_2S partial pressures and operating pressure [4], however, the results in this research were validated with limited field data. Pitting corrosion rate has also been modelled by researchers using damage function analysis by considering pit nucleation, growth rate and re-passivation of carbon steel in chloride solution [22].The pitting rate for underground pipelines was also predicted with lognormal linear model in consideration of environmental variables [29] and the time of

initiation of pitting has also been predicted for different soil categories using Monte Carlo simulation of field observed soil conditions [10].

The above reviewed literatures show that limited work has been done on Markov modelling of internal pitting corrosion of oil and gas pipelines and the few works are either flawed due to limited field validation data or are not based on pure birth non-homogenous Markov modelling, hence, the need for a holistic field data analysis of pitting rate distribution using a continuous time non-homogenous linear growth pure birth Markov model. Since effective corrosion modelling requires a combination of electrochemical activities relating to water and oxides transport within the metal surface, macro-environment (such as temperature, pH, humidity, salinity, porosity) and external environment (such as rainfall, seasonal rainfall and temperature fluctuations) [30], it is possible to model internal pitting corrosion of oil and gas pipelines by considering the operating conditions of the pipelines and the pit depths at different ages. The present work is aimed at determining the future distribution of pit depths of internally corroded oil and gas pipelines by using non-homogenous, continuous time linear growth pure birth Markov process. A multivariate regression analysis of field data was used in a Monte Carlo simulation framework to estimate the time of initiation of the pitting for different categories of pitting rates based on NACE classification. The work used initial knowledge of pit depth distribution to determine the transition probability function of pit depth growth in future time based on the closed form of negative binomial distribution solution of Kolmogorov's forward equation.

2.0 Finite Markov Chain Modelling of internal pitting corrosion of pipelines

A Markov process has no memory because future events are independent of past ones but dependent on the present event [31] hence, if the pit depth of oil and gas pipeline at time t is represented by (P_d), then the probability at such a time can be written as Equation(3):

$$P\{P_d(t) = i\} = P_i(t), i = 1,2, \dots, N \quad (3)$$

where N represents the number of states the pipeline wall is divided, $P_i(t)$ is the probability that the pit depth is at i^{th} state at time t and can be determined by measuring the pit depth distribution at such a time or by expert knowledge[1,8].

If Figure 1 represents a portion of pipeline with wall thickness (w), the time of pit depth distribution shown as a state space variable is represented with Equation(4):

$$\{P_d(t), t \in T\} \quad (4)$$

It should be noted that the pit depth at any time t is an integral part of the pipeline wall thickness whilst T is the time set for the observation of the pit depth. If small change in the pipeline wall thickness (δw) results in a pit depth at i^{th} state represented by (P_{d_i}), then

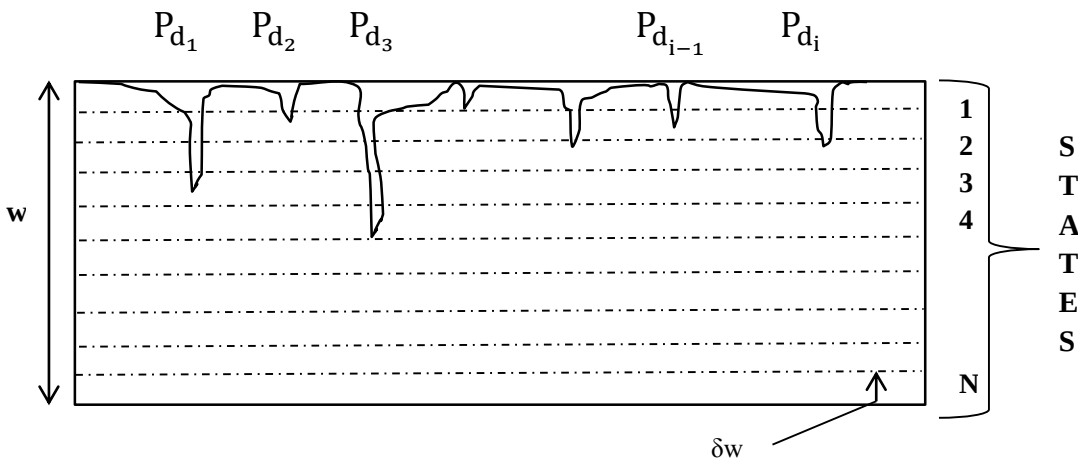

Figure 1: Model of pipeline pitting corrosion

$$\begin{cases} P_d(t) \le P_{d_i} + \delta w \\ P_d(t) > P_{d_i} \\ for\ i = 1,2,\dots,N \end{cases} \tag{5}$$

Assuming P_{d_i} is uniformly distributed with δw corresponding to individual states in the pipeline wall thickness such that the sum of each limit of observable pit depth P_{d_i} is given by $S_{(Pd)_i}$ then

$$P\{P_{d_i}(t) \in S_{(Pd)_i}\} = \begin{cases} P\{P_{d_i}(t) > P_{d_i}\} \\ P\{P_d(t) \le P_{d_i} + \delta w\} \end{cases} \tag{6}$$

It follows therefore that the probability of observed corrosion pit depth at any increase in pipeline wall thickness at time t will satisfy the condition in Equation (7) as shown in literature [13].

$$\begin{cases} 0 \le P\{S_{(Pd)_i}\} \le 1 \\ P\{w\} = 1 \\ P\{\sum_{i=1}^{N} S_{(Pd)_i}\} = \sum_{i=1}^{N} P\{S_{(Pd)_i}\} \end{cases} \tag{7}$$

For any finite collection of time $t_1, t_2, \dots, t_n$ and pit depth , $P_d(t_1), P_d(t_2), \dots, P_d(t_n)$, the time variation of pit depth growth shown in Equation(4) is a stochastic process if the condition in Equation(8) is met.

$$\begin{aligned} P\{P_d(t_{n+1}) = j | P_d(t_n) = i, P_d(t_{n-1}) = i_{n-1}, \dots, P_d(t_0) = i_0\} \\ = P\{\, P_d(t_{n+1}) = j | P_d(t_n) = i\}_{i,j \in N} \end{aligned} \tag{8}$$

where *i* and *j* are variables showing the various state of the pit depth at different times.

2.1 Time Evolution of Pit depth

For transition of the pit depth from state i to j in time interval (t, $t+\delta t$),

$$P\left\{\{[P_d(t+\delta t)=j|P_d(\delta t)=i]=P_{i,j}(\delta t,t)\right\}_{0\le\delta t<t} \tag{9}$$

For the transition probability in Equation (9) to satisfy a Markov process, the condition in equation (10) will hold.

$$\begin{cases} 0 \le P_{ij}(t+\delta t) \le 1, & for \;\; i,j,\delta t,t \ge 0 \\ \sum_{j=1}^{N} P_{ij}(t+\delta t)=1, & for \;\; i,\delta t,t \ge 0 \\ P_{ij}(0,0) = \begin{cases} 1, & for \;\; i=j \\ 0, & for\; i \ne j \end{cases} \end{cases} \tag{10}$$

It is expected that the pit depth in state *i* at a given time δt will remain in the state until a later time [32] however, it can move to another state *j* by passing through an arbitrary state h in s time (see Figure 2) whilst obeying the time-dependent probability condition of Chapman-Kolmogorov equation shown in Equation (11) [32]:

$$P_{ij}(\delta t,t)=\sum_{h=1}^{N} P_{ih}(\delta t,s)*P_{hj}(s,t), \quad for\ \delta t<s<t; s\epsilon(\delta t,t); i,j,h\varepsilon N \tag{11}$$

Assuming that for this small increase in time δt, the probability of transition of the pit depth from state *i* to *j* at time $t+\delta t$ is given by the expression in equation (12).

$$P_{ij}(t,t+\delta t)=\lambda_{ij}(t)\delta t+O(\delta t) \tag{12}$$

where λ is the intensity of the Markov process and can be represented by Equation(13)[32,8].

$$\lambda_i(t)=i\lambda(t) \tag{13}$$

Since $O(\delta t)$ is a limiting state and tends to zero, if a continuous function is assumed such that $\lambda_i(t)\ge 0$, then

$$\begin{cases} \lambda_i(t)=\lim_{\delta t\to 0}\left(\dfrac{1-P_{ii}(t,t+\delta t)}{\delta t}\right) & ,i=1,2,\dots,N \\ \lambda_{ij}(t)=\lim_{\delta t\to 0}\left(\dfrac{P_{ij}(t,t+\delta t)}{\delta t}\right) & ,i,j=0,1,2,\dots,N; i\ne j \end{cases} \tag{14}$$

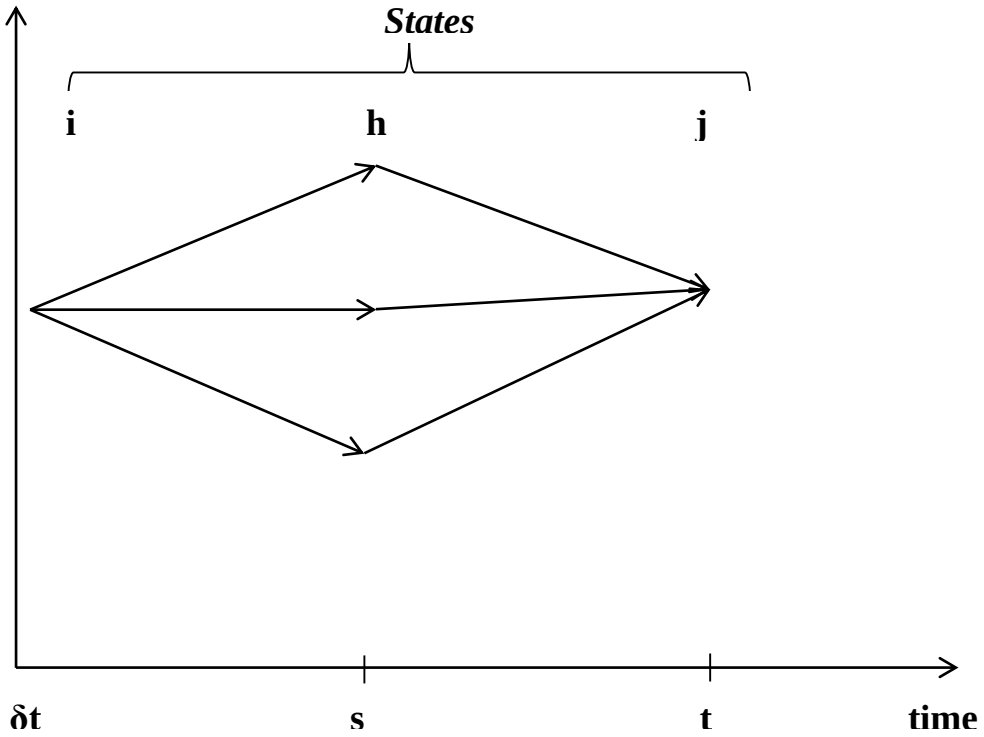

Figure 2: Graphical representation of Chapman-Kolmogorov equation of three stage Markov process [adopted from [32]]

Manipulating Equation (14) will give the Kolmogorov forward and backward equations, however, for a continuous time non-homogenous linear growth Markov process which the pit depth is assumed to follow in this research, the probability that a process at state i will be in state j for $j \geq i$ at a later time follows Kolmogorov forward equation shown in Equation (15) [1, 8, 13].

$$\frac{dP_{ij}(t)}{dt} = \begin{cases} \lambda_{j-1}(t)P_{i,j-1}(t) - \lambda_j(t)P_{i,j}(t), & for\ j \geq i+1 \\ -\lambda_i(t)P_{i,i}(t) \end{cases} \tag{15}$$

The transition probability function of the pit depth defined by Kolmogorov forward equation can be solved with a negative binomial distribution function [1,6, 8]hence the conditional probability (P_{n,n_0}) of moving from state n_0 to n ($n \geq n_0$) in time interval (t_0,t) can be represented with the relationship in Equation (16).

$$P_{n,n_0} = P\{P_d(t) = n | P_d(t_0) = n_0\} \tag{16}$$

Parzen [33] showed that Equation (16) can be represented in a closed form of negative binomial distribution (Equation(17)) for the distribution of pit depths with initial state n_0 and n being the probability density of the smallest and deepest pit depths respectively of the pipeline at time t_o.

$$P_{n,n_0} = \binom{n-1}{n-n_0} * e^{-(\gamma(t)-\gamma(t_0))n_0} * \left(1 - e^{-(\gamma(t)-\gamma(t_0))}\right)^{n-n_0} \tag{17}$$

where ,

$$\gamma(t_0, t) = \int_{t_0}^{t} \lambda(t)dt \tag{18}$$

The time-dependent pit depth growth can be expressed as a function of the intensity of the Markov process and change in time Δt [34] as shown in Equation (19):

$$P_d(t + \Delta t) = P_d(t) + P_d(t) * \lambda \Delta t \tag{19}$$

Since

$$\frac{d(P_d(t))}{dt} = \lim_{\Delta t \to 0} \frac{P_d(t + \Delta t) - P_d(t)}{\Delta t} \tag{20}$$

Solving Equation (19) and (20) will yield the non-probabilistic pit depth (Equation (21)) at any change in time interval ($\Delta t = t - t_0$) assuming that the pit depth at time t_0 is in the initial state n_0.

$$P_d(t) = n_0 e^{\lambda \Delta t} \tag{21}$$

The time dependent stochastic mean pit depth growth (*M (t)*) is equivalent to the non-probabilistic pit depth and can be expressed as follows:

$$M(t) = n_0 e^{\lambda (t - t_0)} \tag{22}$$

If the deterministic corroded pit growth in this work is assumed to follow a linear random model which have been used by researchers to model different kinds of physical systems including pipelines deterioration [26, 35-38], then the progression of the deterministic pit depth ($P_{d_d}(t)$) will be of the form shown in Equation (23).

$$P_{d_d}(t) = \beta_d (t - t_{int}) \tag{23}$$

where β_d represents the deterministic pitting rate, t_{int} is the time of initiation of the pitting process (this is explained later in this work). The time of pitting initiation on the pipeline depends on the physical and chemical characteristics of the environment exposed to the pipeline [10, 30] and the corrosion resistance ability of the pipeline material. The rate of change of deterministic pit depth ($\Delta P_{d_d}(t)$) can be expressed in terms of the deterministic intensity (λ_d) and change in time interval as follows:

$$\Delta P_{d_d}(t) = \lambda_d(t) P_{d_d}(t) \Delta t \tag{24}$$

According to Cox and Miller (1965) (as cited by Valor *et al.* [1]) the stochastic corroded pit growth rate is assumed to be equal to the deterministic pit growth rate. Then solving Equations (18), (22) and (24) and simplifying will yield the following relationships:

$$\gamma(t) = ln(\beta_d (t - t_{int})) \tag{25}$$

$$\lambda(t) = \frac{1}{t - t_{int}} \tag{26}$$

$$\gamma_s = \frac{t_0 - t_{int}}{t - t_{int}} \quad , t \geq t_0 \geq t_{int} \tag{27}$$

Where $\gamma(t)$ represents the pitting corrosion damage with time whilst γ_s represents the probability of pitting evolution with time.

2.2 Estimation of the Probability Distribution of the Corroded pitting depth

Caleyo et al. [12] has shown that the probability distribution (*FD (π)*) over the time interval (*t, t_0*) at state *n_0* can be related to the probability density function (*f (π)*) according to Equation (28):

$$FD(\pi) = \int_{t_0}^{t} f(\pi), t > 0 \tag{28}$$

If the pitting corrosion rate (π) is continuously distributed with *f (π)*, *FD (π)* and *Δt*, then Equation (28) can be expressed below after taking the limiting states and simplifying:

$$P\{\pi(t) < T \leq \pi(t) + \pi(\Delta t)\} \cong f(\pi) * \Delta t \tag{29}$$

$$f(\pi, n_0, t_0, t) = P_{n_0}(t_0) * P_{n_0, n_0+\pi\Delta t}(t_0, t) * \Delta t \tag{30}$$

For an oil and gas pipeline with a measured total pitting population, the pitting distribution for the entire pitting states (*N*) of the pit depths can be expressed as Equation (31):

$$f(\pi, t_0, t) = \sum_{n_0=1}^{N} f(\pi, n_0, t_0, t) \tag{31}$$

Different researchers have shown that if the initial probability distribution of the pit depth at time t_0 is known, the future probability distribution of the pit depth can be estimated [1, 6, 8, 12] and reliability of the pipeline established. Equation (32) is used to compute the future distribution of the pit depth (*P_n (t)*) [19].

$$P_n(t) = \sum_{n_0}^{n} P_{n_0}(t_0) * P_{n_0,n}(t_0, t) \tag{32}$$

Combining Equations (17), (25), (26) and (32) will give a general equation for determining the future pit depth distribution.

$$P_{n_0,n}(t_0,t) = \frac{(n-1)!}{(n_0-1)!\,(n-n_0)!} * \left(\frac{t_0 - t_{int}}{t - t_{int}}\right)^{n_0} * \left(\frac{t - t_0}{t - t_{int}}\right)^{n-n_0} \tag{33}$$

3.0 Prediction of the Model parameters

To predict the transition probabilities for the deterministic pit depth requires the estimation of the deterministic pitting rate and the time of initiation of the pitting in Equation (23). To estimate these parameters, pit depths and operating parameters (pH, temperature, flow rate and CO_2 partial pressure) measurements of oil transmission pipelines obtained from a producing company in Nigerian Niger Delta region were used for numerical analysis and determination of the multivariate coefficients following the Monte Carlo framework shown in Figure 3.

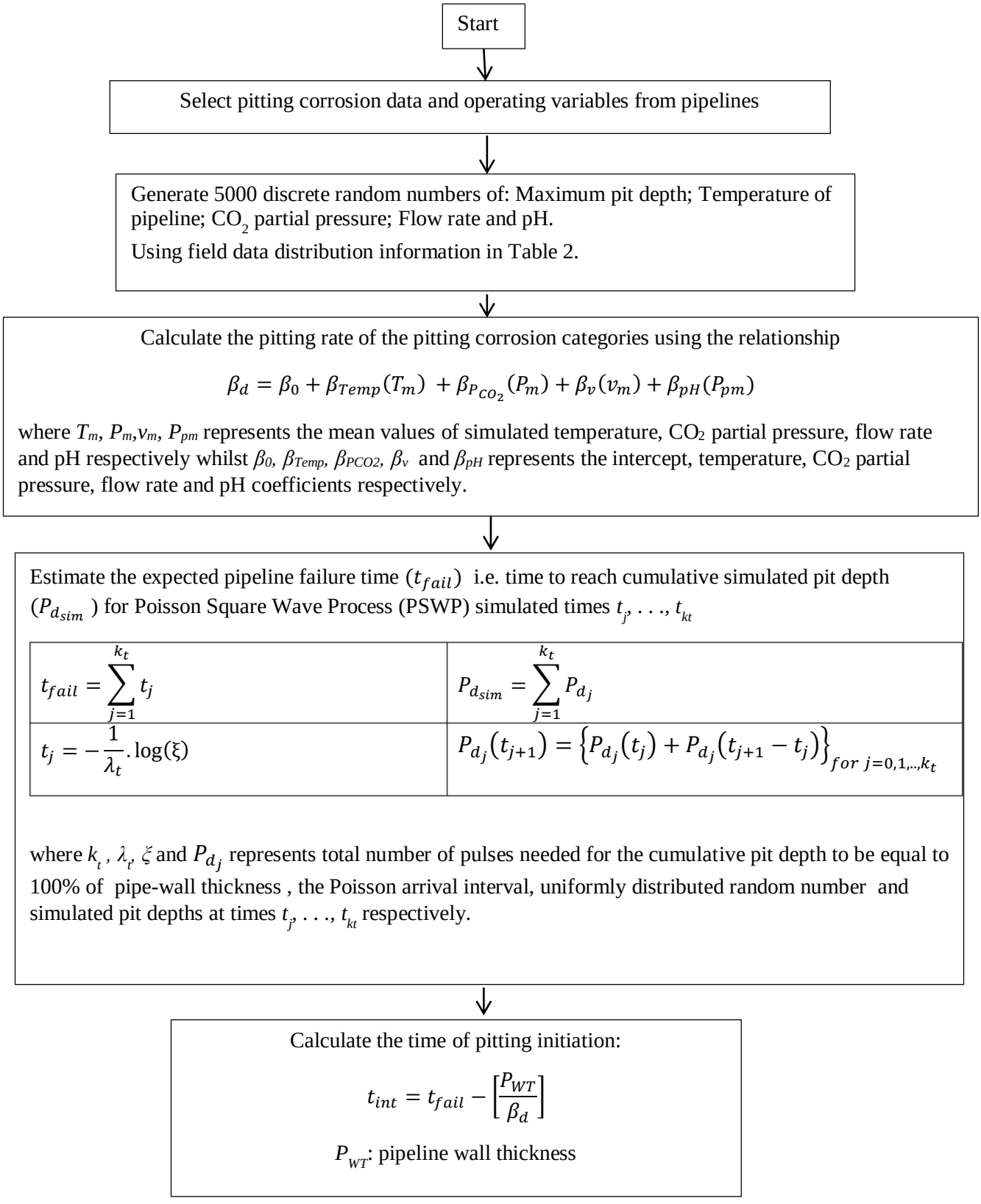

Figure 3: framework for Monte Carlo simulation of pitting initiation time

The pitting rates in the pipelines were classified into four categories using NACE pitting corrosion guideline shown in Table 1 [39].

Table1: Qualitative categorization of carbon steel corrosion rate for oil production systems

	Average Corrosion Rate	Maximum Pitting Rate
	mm/yr	mm/yr
Low	<0.025	<0.13
Moderate	0.025-0.12	0.13-0.20
High	0.13-0.25	0.21-0.38
Severe	>0.25	>0.38

The pit depths of the pipelines were determined according to the relationship in Equation (34)-(36):

$$P_{d_{max}} = \left\{\left(\beta_0 + \sum_{i=1}^{m} \beta_i x_i\right)(t_i - t_{int})\right\}_{i=1,2,\ldots,m} \quad (34)$$

where

$$\beta_d = \left\{\beta_0 + \sum_{i=1}^{m} \beta_i x_i\right\}_{i=1,2,\ldots,m} \quad (35)$$

$$\beta_d = \beta_0 + \beta_{Temp}(T_m) + \beta_{P_{CO_2}}(P_m) + \beta_v(v_m) + \beta_{pH}(P_{pm}) \quad (36)$$

$P_{d_{max}}$ represents the maximum pit depth which is equivalent to the deterministic pit depth ($P_{d_d}(t)$), β_i represents the coefficients of the operating variables of the pipelines and x_i is used to represent the operating variables whilst m is the number of operating variables.

To ensure that the random walk nature of the pit depth growth rate is maintained, a Poisson Square Wave Process (PSWP) was used to predict the time lapse for the pitting process. Although any positive random distribution can be used for realizing the pulse heights [26], Gamma distribution [26] as well as Gumbel distribution [25] have been used for estimating variables in PSWP by other authors, however, lognormal distribution is employed in this work because the best fitting distribution of the field data followed a lognormal distribution. In order to estimate the time of pitting initiation process (t_{int}) using the procedure shown in Figure 3, a 5000 run random numbers simulation was carried out using the minimum and maximum values of the operating variables and the maximum pit depths for the corrosion categories shown in Table 2 as boundary conditions. By assuming that the maximum pit depth and operating parameters follows a lognormal distribution as earlier stated, the best fit distributions were obtained from the simulated data whilst a Poisson Square Wave Process (PSWP) shown in Figure 4 was used to calculate the pit depth growth with time using the relationship shown in Equation (37) [26].

$$P_{d_j}(t_{j+1}) = \left\{P_{d_j}(t_j) + P_{d_j}(t_{j+1} - t_j)\right\}_{for\ j=0,1,..,k_t} \quad (37)$$

where P_{d_j} represents the simulated pit depth at time t_j and k_t represents the expected number of time pulses needed for the cumulative pit depth to be 100% of the pipe-wall thickness. A multivariate regression analysis of the simulated data was used to obtain the regression coefficients of the operating variables and the intercept whereas the mean values of the operating

parameters computed from the simulation result were used for the computation of the pitting rates of the corrosion categories according to Equation (36).

To estimate the excepted pipeline failure time (t_{fail}), Poisson arrival rate (λ_t) was assumed to be 0.5 and the statistical best fit parameters of the lognormal distribution estimated from the 5000 simulation runs were used to predict pit depth for random times calculated for each Poisson arrival. Since the magnitude and duration of the generated pulses from the PSWP follow a Poisson distribution with the duration of individual pulses being independently exponentially distributed [25-26], the excepted pipeline failure time (t_{fail}) can be computed as the cumulative simulated times for which the cumulative simulated pit depth ($P_{d_{sim}}$) is equivalent to 100% of the pipe-wall thickness of the pipeline.

As the deterministic pit depth at the expected time of pipeline failure (t_{fail}) is assumed to be equivalent to 100% of the pipe-wall thickness (P_{WT}) loss, then Equation (23) can be represented as shown in Equation (38) if $t \approx t_{fail}$.

$$P_{WT}(t_{fail}) = \beta_d(t_{fail} - t_{int}) \tag{38}$$

Hence the pitting initiation time can be simply simplified from Equation (38) to give the relationship expressed in Equation (39) at the time of failure of the pipeline.

$$t_{int} = t_{fail} - \left[\frac{P_{WT}}{\beta_d}\right] \tag{39}$$

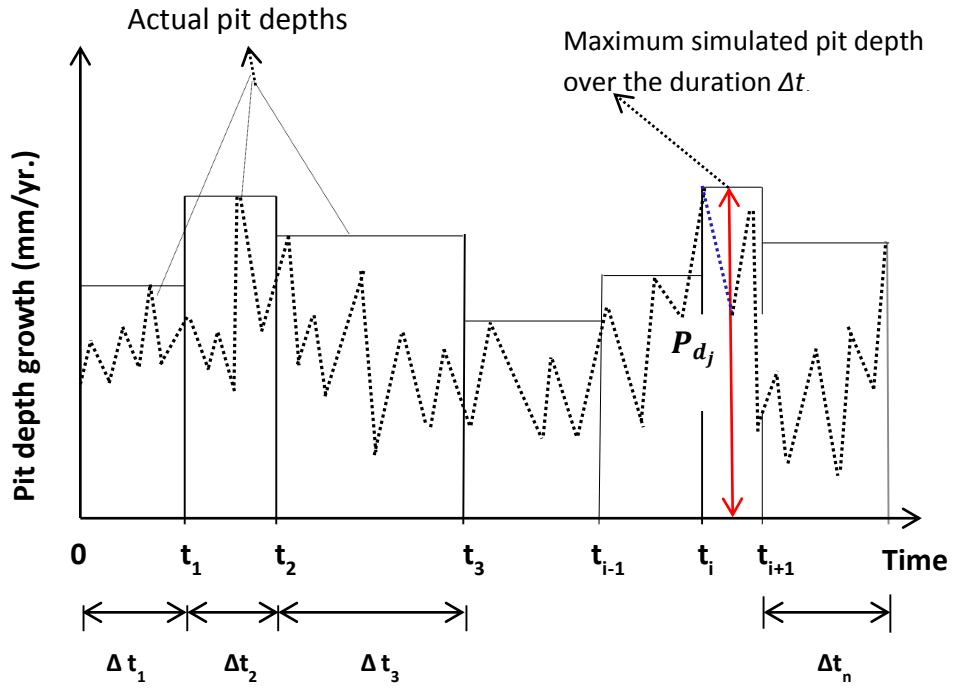

Figure 4: Poisson Square wave Process (PSWP) for estimating pitting initiation time

The summary of the field data for the pitting corrosion categories, the coefficients of regression for the linear regression model and Monte Carlo simulation predicted values of time for pitting initiation is shown in Table 2. In the table, "all data" category represents the total number of collected data whereas low, moderate, high and severe pitting rate categories were determined according to the number of all the

sampled data that fell into the classifications shown in Table 1. After the simulation and estimation of the relevant variables in Equation (34), the transition probability function given in Equation (33) can be calculated for the pitting corrosion categories.

Table 2: Variables and coefficients of the predictive for the pitting corrosion

Variables		Description	Pitting corrosion category				
			Low	Moderate	High	Severe	All data
$P_{d_{max}}$	min	Maximum pitting depth (mm)	0.049	0.132	0.204	0.396	0.049
	max		0.118	0.183	0.371	1.309	1.309
ϑ	min	Temperature (^{0}C)	24	21	27	21	21
	max		40	32	70	74	74
P_{CO2}	min	CO_2 partial pressure (MPa)	0.01	0.01	0.02	0.03	0.01
	max		0.14	0.16	0.31	0.61	0.61
V	min	Flow rate(ms^{-1})	0.07	0.04	0.05	0.07	0.04
	max		0.23	0.3	1.39	2.01	2.01
p_H	min	pH of fluid	6.21	6.78	6.21	6.73	6.21
	max		8.18	8.32	8.19	8.57	8.57
No of sampled pipelines			8	7	15	30	60
No of sampled pit depths			80	70	150	300	600
		Coefficient of parameters					
β_0	Constant pitting rate		0.0836	0.1574	0.2859	0.8235	0.7303
	Standard error		0.0029	0.00278	0.0064	0.037	0.042
	Coefficient of temperature		-0.0001	-0.0001	-0.0001	-0.0002	-0.0002
β_{Temp}	Standard error		4.24e-05	4.24e-05	3.82e-05	0.0002	0.0002
	Coefficient of CO2 partial pressure		-0.003	-0.0019	-0.0033	0.0133	-0.0279
β_{PCO2}	Standard error		0.0053	0.0034	0.0057	0.0157	0.021
β_V	Coefficient of flow rate		0.0002	-0.0001	-0.0001	-0.0026	0.0038
	Standard error		0.0042	0.0019	0.0012	0.0047	0.006
β_{pH}	Coefficient of pH		0.0003	0.0003	0.0007	0.0046	-0.0049
	Standard error		0.0003	0.0003	0.0008	0.0049	0.005
		Estimated pitting parameters					
β_d	Pitting rate (mmyr^{-1})		0.0824	0.1568	0.2855	0.8506	0.6801
t_{int}	pit initiation time(years)		1.56	0.58	1.03	1.89	3.60

4.0 Results and Discussion

The minimum and maximum observed pit depths of each of the 60 pipelines were used as boundary conditions for a Monte Carlo simulation experiment aimed at predicting the variation of the pit depth growth with time of exposure of the pipelines for different categories of pitting rate shown in Table 1. This simulation executed in Matlab was used to obtain results for 1 year to 40 years exposure of the studied pipelines. The cumulative simulated pit depths for each of the simulated exposure years (5, 10, 15, 20, 25, 30, 35 and 40 years) for the 60 pipelines were ranked in increasing order and the pit depth of each pipeline plotted against the ranked position. The distribution of the simulated pit depths for all the field data and the best fit equations for the exposure times are shown in Figure 5.

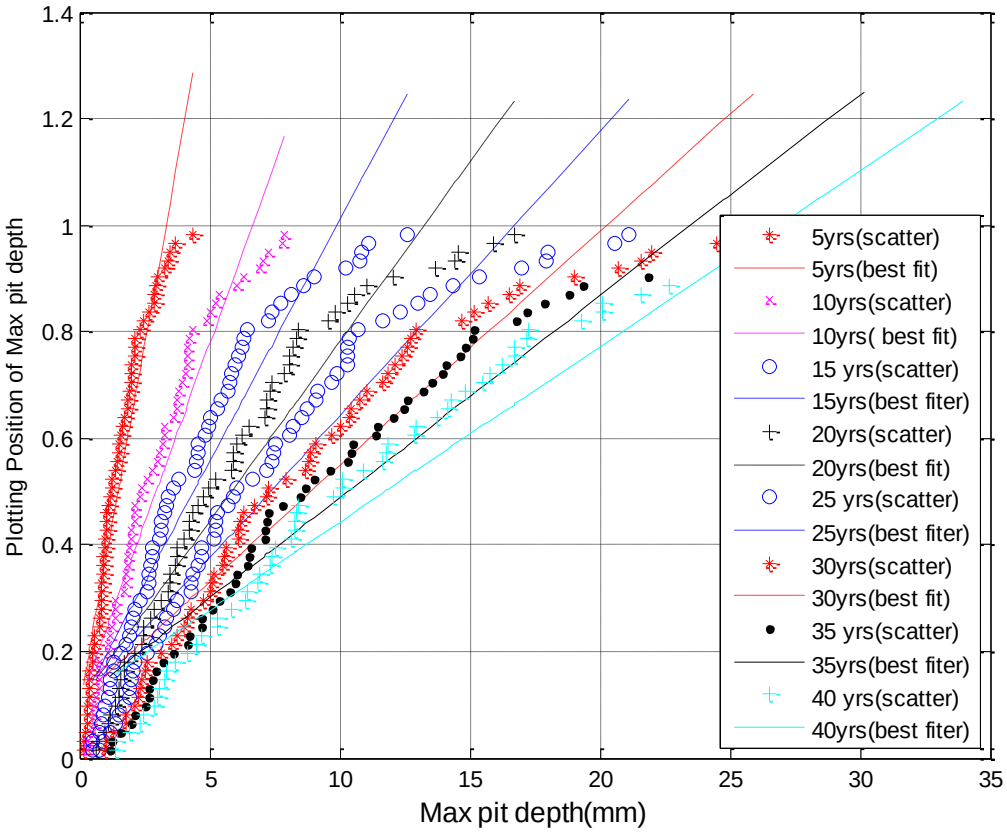

Figure 5: Maximum pit depth plot for Monte Carlo simulated maximum pit depths for studied pipelines

Figure 5 shows that the distributions were shifting towards the right in a clockwise direction as the values increased, which is an indication of experiment under control [28]. The trend shown in Figure 5 is similar to those of the simulated pit depth growth of the pitting corrosion categories not shown in this paper.

The simulated pit depths and the exposure times for the pitting corrosion categories were fitted to the generalized extreme value (GEV) distribution shown in Equation (40).

$$f(x) = Exp\left[-\left(1+\sigma\frac{x-\varphi}{\alpha}\right)^{-\frac{1}{\sigma}}\right] \quad for\ \left(1+\sigma\frac{x-\varphi}{\alpha}\right) > 0 \qquad (40)$$

where *f(x)* represents the GEV distribution, σ is the shape parameter, φ is the location parameter, α is the scale parameter.

Figure 6a shows the GEV distribution of the simulated data for the entire field data used in this research. The pitting depth states were obtained by dividing the pipeline wall thickness into 100 states of 0.0841 mm-thick with each state representing a damage penetration of the pipeline wall in the discretization process. The figure indicates that the variance and the mean of the pitting rate distribution decrease with the increase in time of exposure.

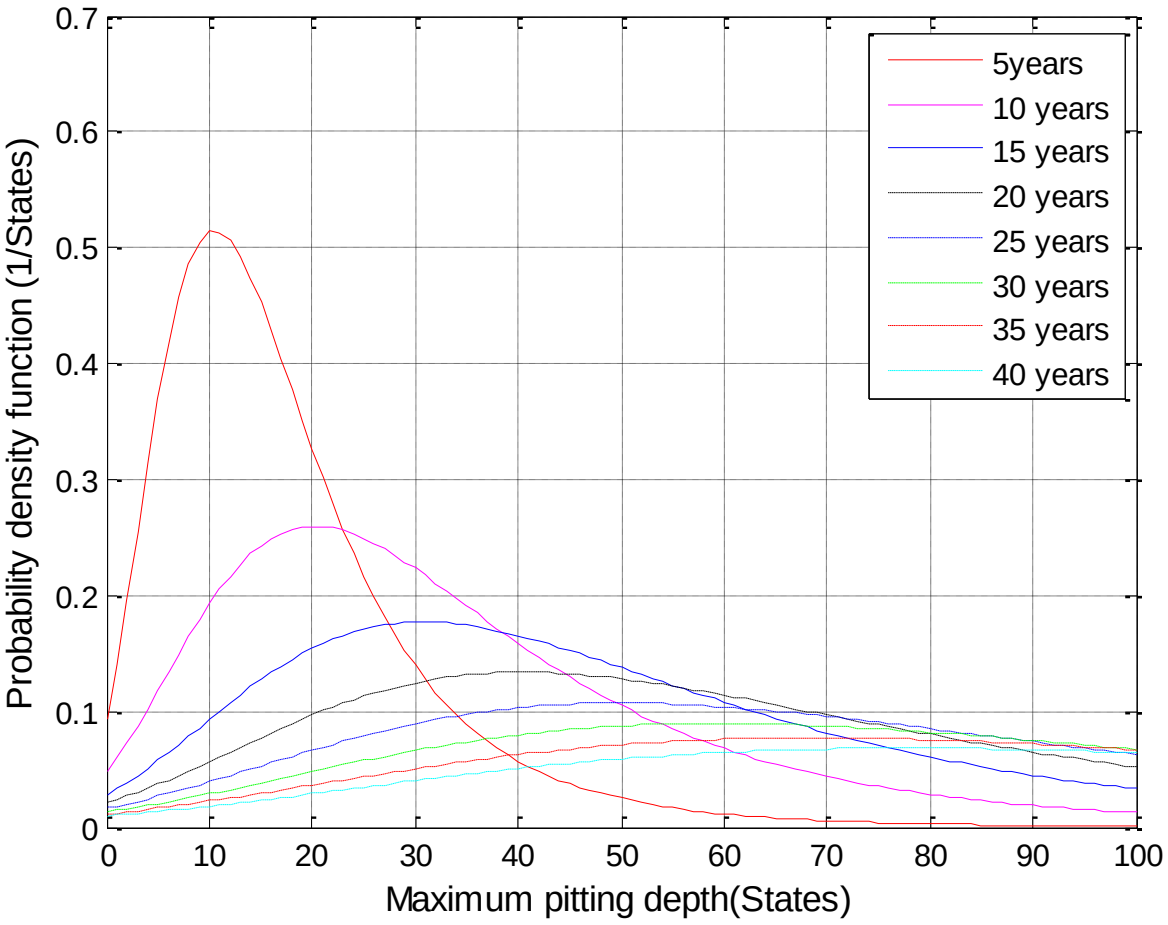

Figure 6a: GEV distribution of Monte Carlo simulated pit depth for all pitting corrosion data

The stochastic internal pit depth growth was illustrated in Figure 6b using Monte Carlo simulated pit depth growth shown in Figure 6a. The pit depth distribution at 5 years was used for constructing the future pit depth distribution at 10 years, 15 years and 20 years as the pipeline wall thickness was divided into 100 states of 0.0841 mm-thick per state. The constructed pit depth distribution shown in Figure 6b indicated that the pitting rate distribution decreased with the increase in time of exposure as was concluded by other researchers [1, 12].

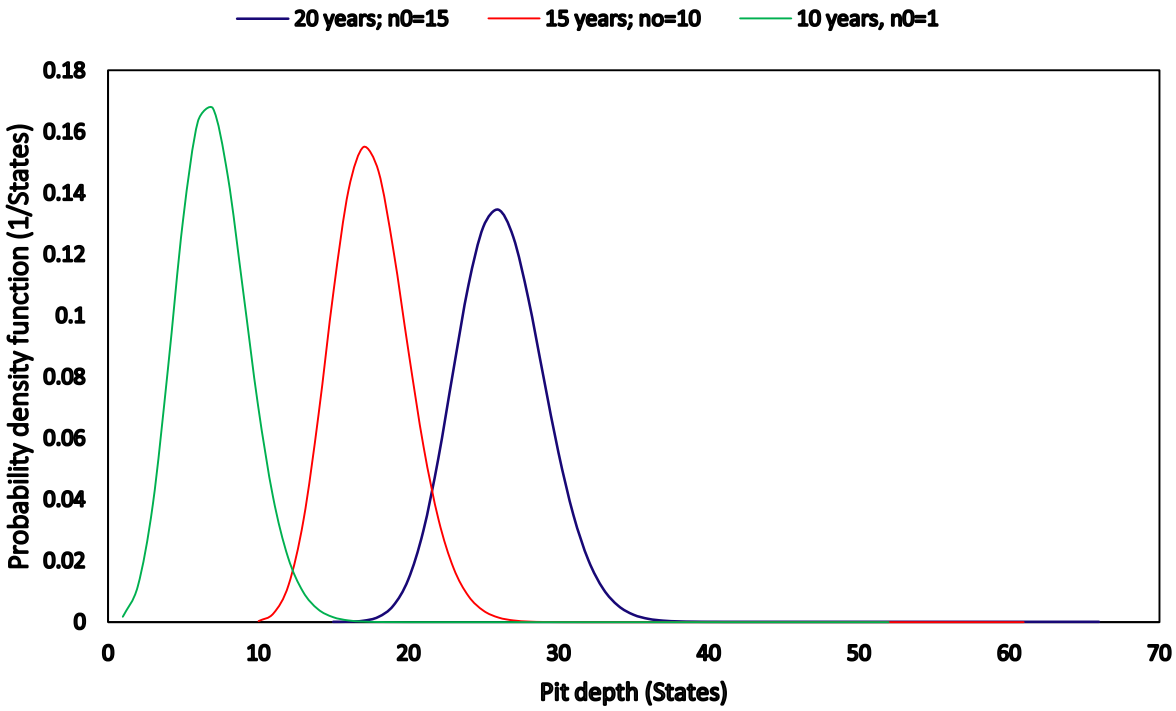

Figure 6b: Variation of pitting depth distribution with pipeline exposure time (years)

Figures 7a and 7b represent the mean and variance of the simulated pit depths over different times of exposure. The figures indicate an increase in mean and variance of the pitting corrosion categories as the time of exposure increased. It could also be seen that severe pitting and 'all data' categories have higher values and showed more scatter than low, moderate and high pitting corrosion classes. This implies that the increase in pit depths resulted in higher mean and variance for pipelines with the same duration of exposure.

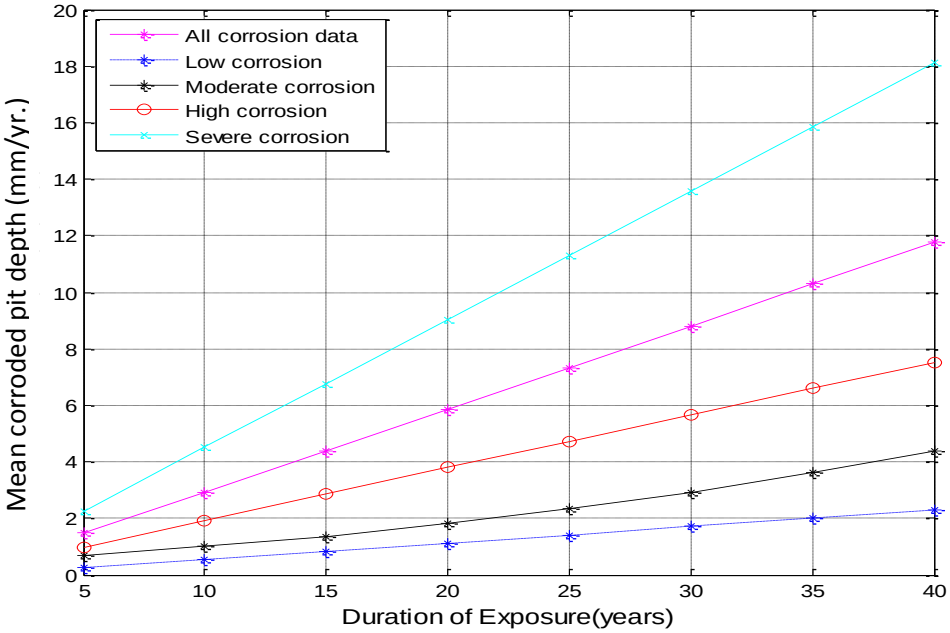

Figure 7a: Time evolution of the best fit mean of Monte Carlo simulated pit depth

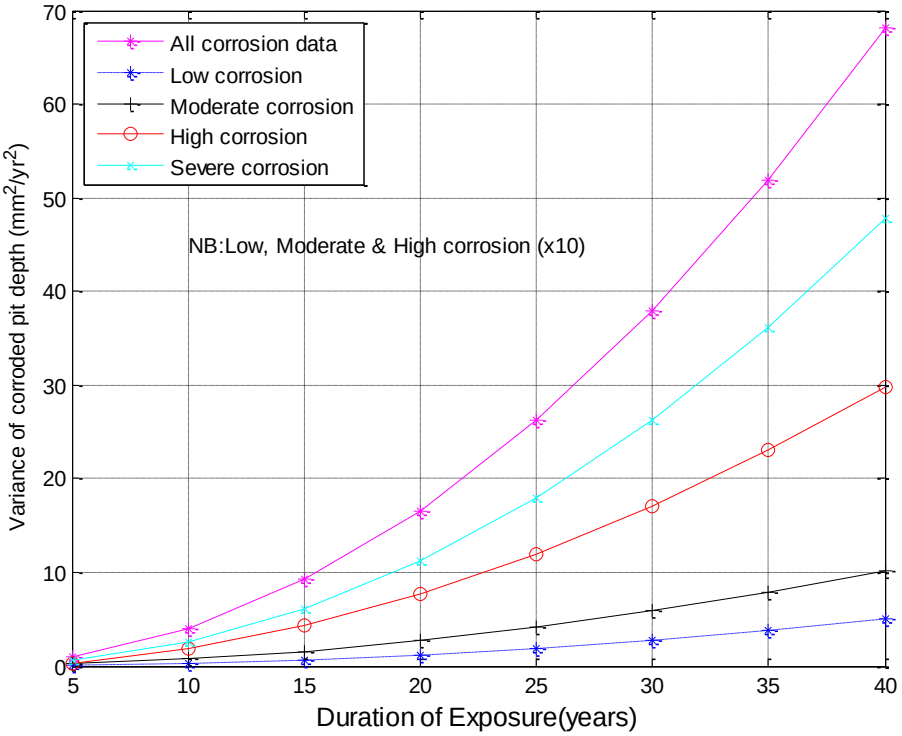

Figure 7b: Time evolution of the best fit variance of Monte Carlo simulated pit depth

Figures 8a, 8b and 8c represent the variation of the shape, scale and location parameters of the pitting corrosion categories for the simulated data. As expected, there is increase in these variables with increased

duration of exposure with low, moderate and high categories giving lower values of the scale and location parameters whilst shape parameters showed slight changes for high, severe and all data .

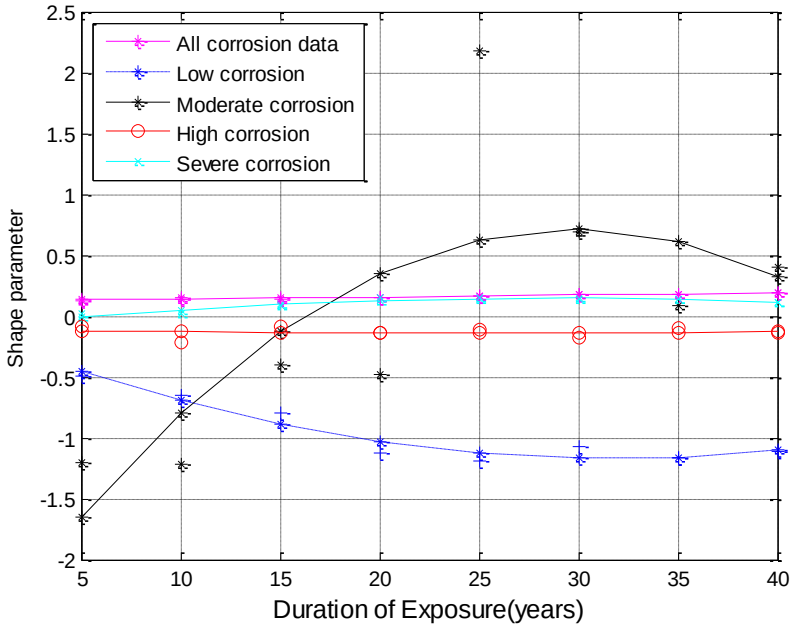

Figure 8a: Time evolution of the best fit shape parameter of GEV distribution of the pit depth

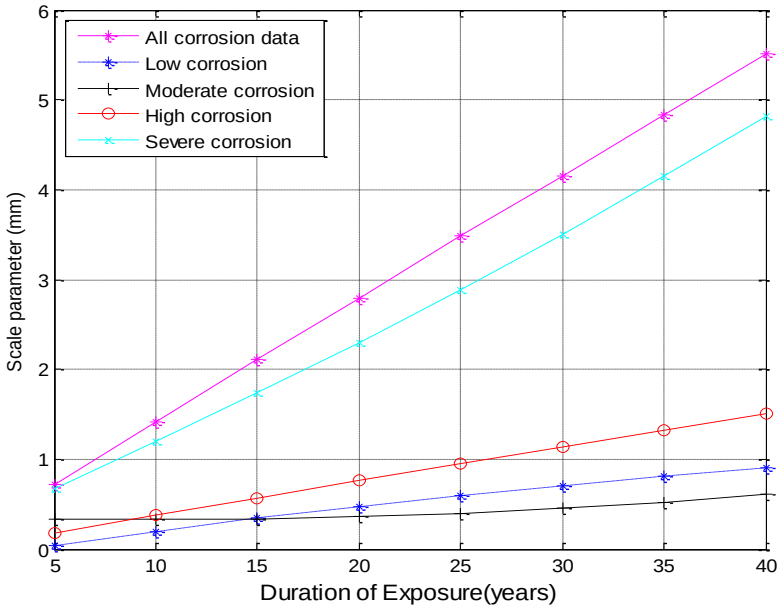

Figure 8b: Time evolution of the best fit scale parameter of GEV distribution of the pit depth

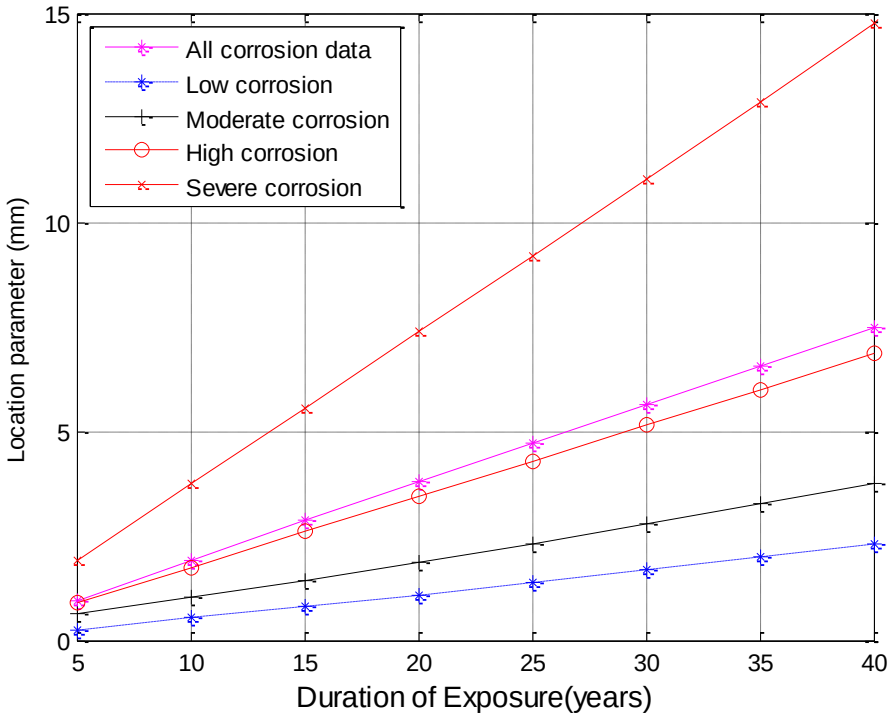

Figure 8c: Time evolution of the best fit location parameter of GEV distribution of the pit depth

The variation of the pitting damage ($\gamma(t)$) and the probability parameter (γ_s) with time is also shown if Figures 9a and 9b respectively whereas Figure 9c shows the maximum pit depth growth with time as computed from the simulation result. The estimation of these parameters is vital for the computation of the transition probability function. The pitting corrosion damage increased with time as expected, with the least increase observed in low pitting corrosion category whereas severe pitting corrosion category accounted for the highest increase as was concluded by other researchers [1, 8]. Since higher pit depths resulted in lower probability parameter (Figure 9b), it follows that the reliability of the pipeline reduces with an increased risk of failure as exemplified by other authors in literature [9, 27].

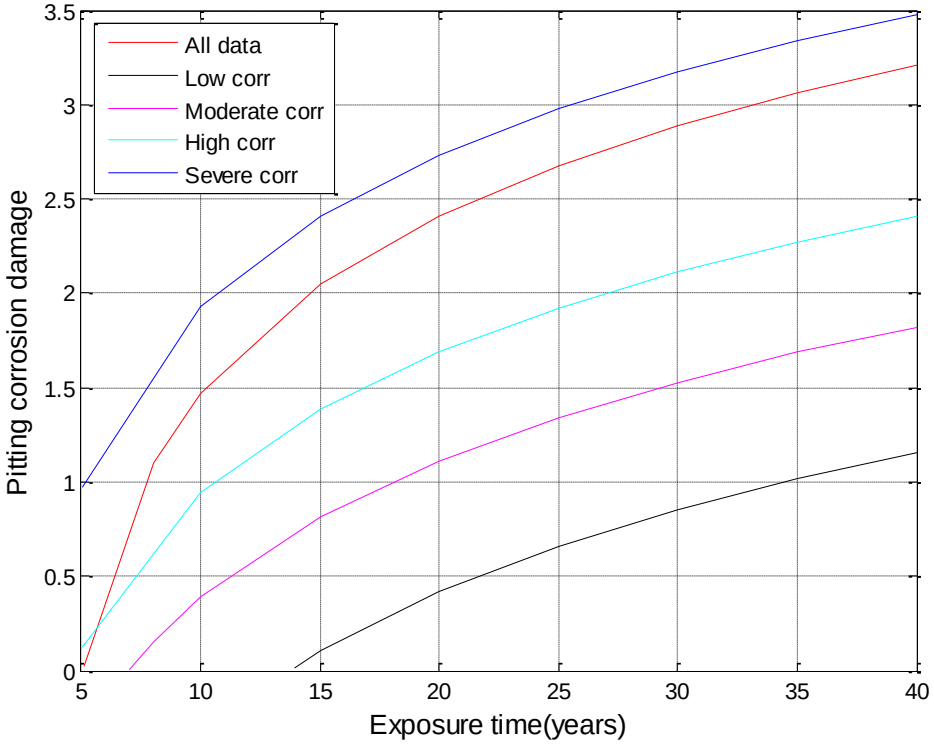

Figure 9a: Time evolution of the pitting corrosion damage (ϒ (t)) for GEV distribution of Monte Carlo simulated pit depth for different categories of pitting corrosion

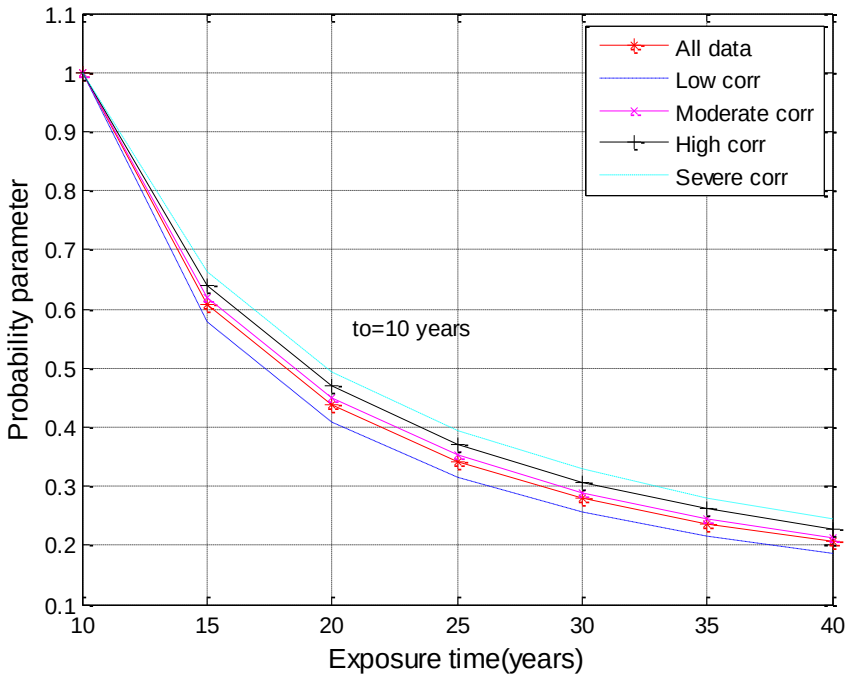

Figure 9b: Time evolution of probability parameter (Υ_s) for GEV distribution of Monte Carlo simulated pit depth for different categories of pitting corrosion

Figure 9c indicates that the cumulative rate of growth of the pit depth is maximum for severe corrosion rate as expected whereas low corrosion category showed the least cumulative pit growth with time of

pipeline exposure. Hence, to manage pipelines with these corrosion severities involves the application of varying quantities of corrosion inhibitors, however, if the maximum uninhibited corrosion rate is less than 0.4mm/yr., there may not be any need for corrosion inhibitor seeing that this level of pipe-wall thickness loss is accommodated in corrosion allowance during pipeline design [40]. Although the pipelines studied in this work were treated with imidazoline-based corrosion inhibitor, however, to reduce the risk of pipeline failure due to corrosion rates greater than 0.4mm/yr., varying quantities of corrosion inhibitors are injected to the pipelines in accordance to the rate of corrosion. For instance, when the total uninhibited corrosion rate on a carbon steel pipeline is 0.7mm/yr., the maximum required inhibitor availability will be 50% [40]. Again, the concentration of the inhibitor is also vital in achieving the expected corrosion reduction seeing that at certain concentrations, corrosion is enhanced. This is evident in X52 grade pipeline which showed perfect corrosion reduction at 50ppm of amine type inhibitor but increased corrosion rate at 100 ppm under static condition [41]. This inhibitor application can be periodically reviewed after inspection of the pipelines to determine whether or not the quantity is sufficient or in excess. Imperatively, the quantity of corrosion inhibitor to be applied to the pipelines studied in this research will increase from low corrosion to moderate, high and severe corrosion categories in that order of listing. Again, the pipelines with higher pit depth growth rates are expected to continue growing at a higher pace than those with lower pitting rates hence, the failure risk expected for severe corroded pipelines are much higher than the risk inherent in low corroded pipeline.

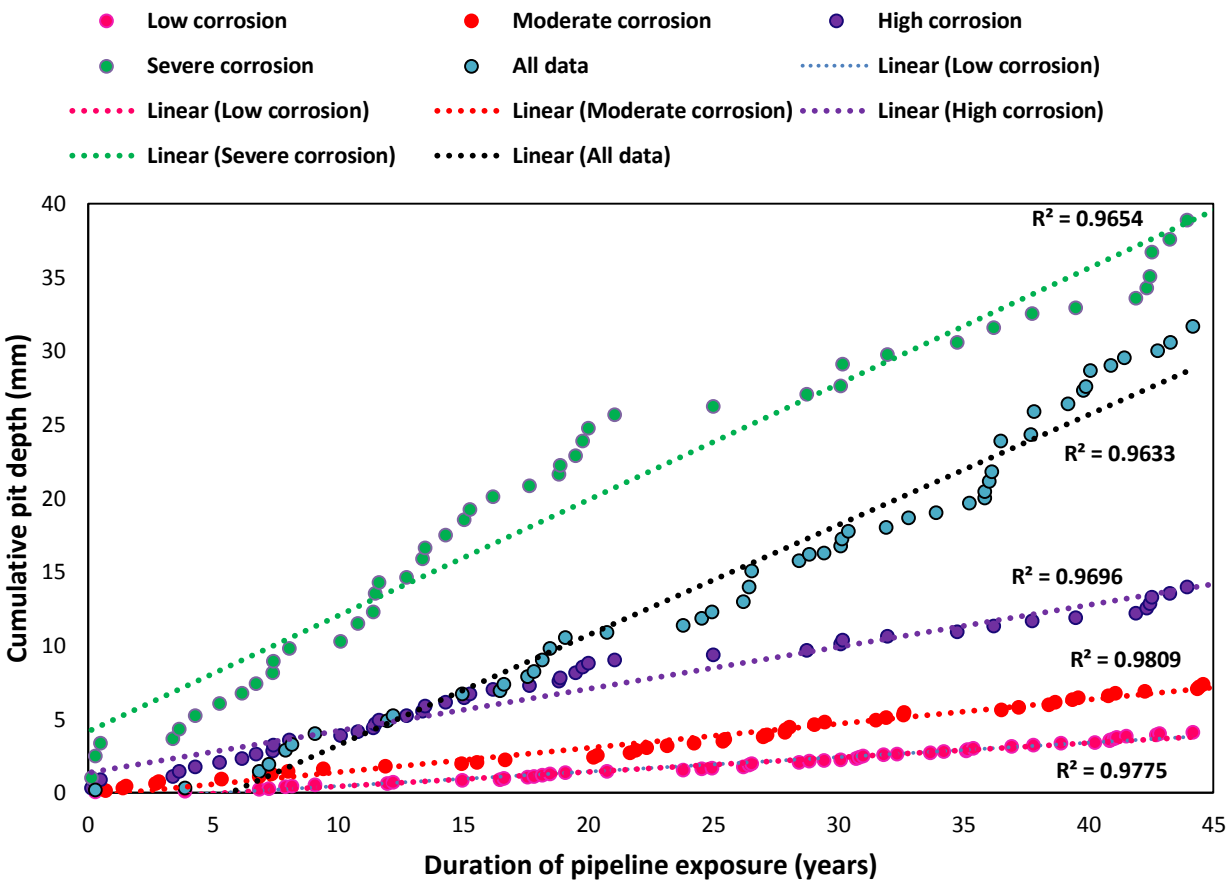

Figure 9c: Simulated maximum pit depth growth and pipeline exposure time for different corrosion categories.

4.1 Applications of the Pitting Prediction Model

The Markov prediction model was tested on two sets of in-line inspection data of pit depth of offshore well tubing and onshore transmission pipelines.

4.1.1 Predicting Future Pitting Corrosion Distribution of Well Tubing

The proposed Markov model was used to predict the future pitting corrosion distribution of well tubes used for offshore production. The pit depths of these tubes were measured with Multi-finger Imagining Tool (MIT). The summary of the pit depths, the ages and the frequency of occurrences of the field measured data can be found in reference [42]. The pit depth frequency of occurrence was used to determine the transition probability function of the pit depths that were divided into 100 states of 0.0645 mm-thick per state. To apply the Markov prediction model, the pit depths were assumed to belong to all data category (see Table 2) with pitting initiation time of 3.6 years.

For L-80 grade steel well tubing, the initial probability distribution function was taken as the pit depth distribution at age 5.1 years whilst the future pit depth distribution was calculated for 5.8 years and the result compared with the field measured pit depth distribution at 5.8 years. The result of the field measured and Markov predicted pit depth distribution is shown in Figure 10. The field and Markov predicted pit depth distributions were subjected to two-sample Kolmogorov Smirnov (K-S) test to prove the hypothesis that Markov predicted distributions of L-80 grade carbon steel's pit depth is similar to the future field measured pit depth distribution in offshore location. The resulting p-value of 0.4496 from the K-S test shows that this hypothesis cannot be rejected.

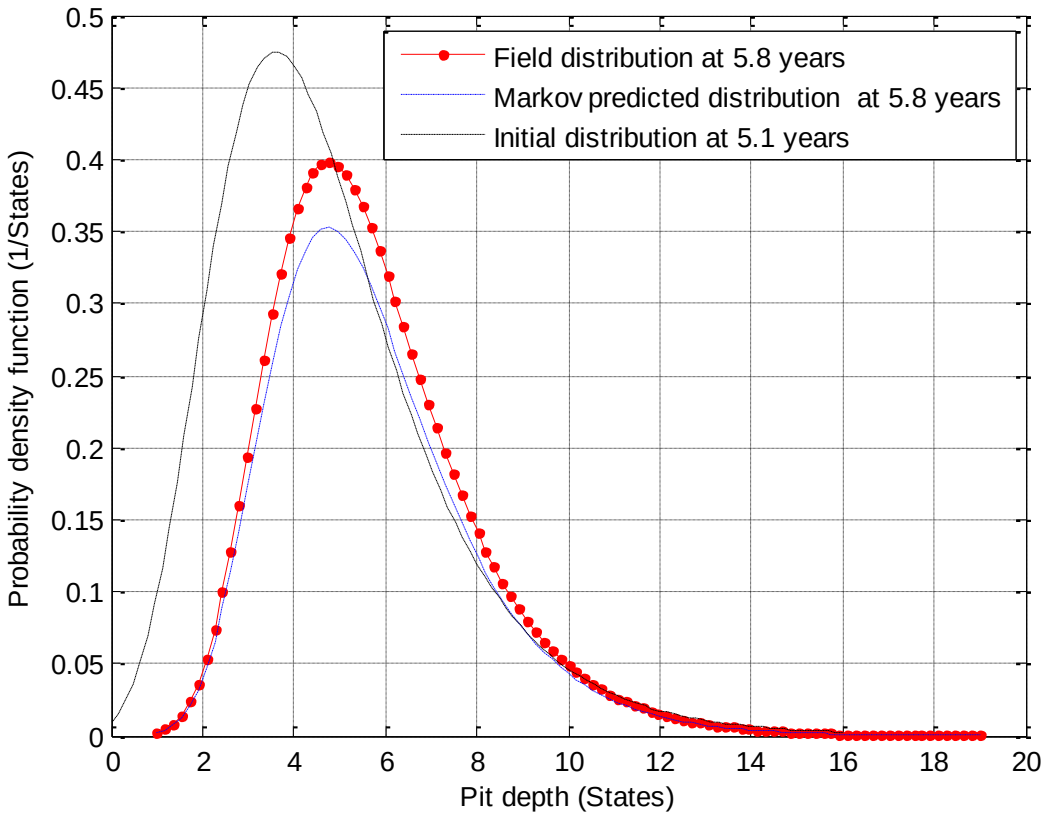

Figure 10: Comparison of Markov model prediction and field measured pit depths distribution for L-80 grade well tubing at 5.8 years from initial field distribution at 5.1 years

Similarly, for the N-80 grade carbon steel well tubing, the initial pit depth at the age of 9.1 years was used as the initial transition probability function distribution for calculating the future pit depth distribution at 15.3 years, 18.2 years and 22.8 years. The results of the Markov predicted and field measured pit depth distribution is shown in Figures 11a, 11b and 11c. Again, a two-sample K-S test of the Markov and field measured pit depth were conducted to test the hypothesis that Markov predicted distributions of N-80 grade carbon steel's pit depth is similar to the future field measured pit depth distribution in offshore location. The p-values of 0.1976, 0.1438 and 0.1024 for 15.3 years, 18.2 years and 22.8 years respectively were enough not to reject the hypothesis.

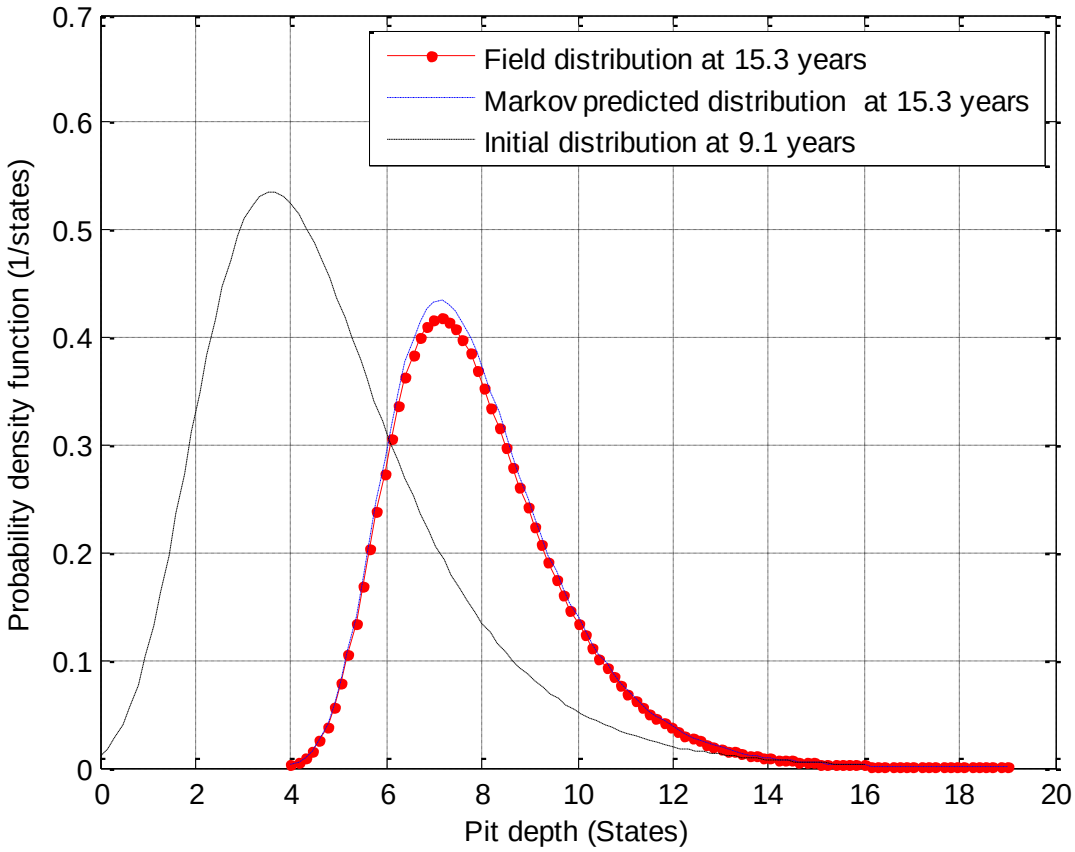

Figure 11a: Comparison of Markov model prediction and field measured pit depths distribution for N-80 grade well tubing at 15.3 years from initial field distribution at 9.1 years

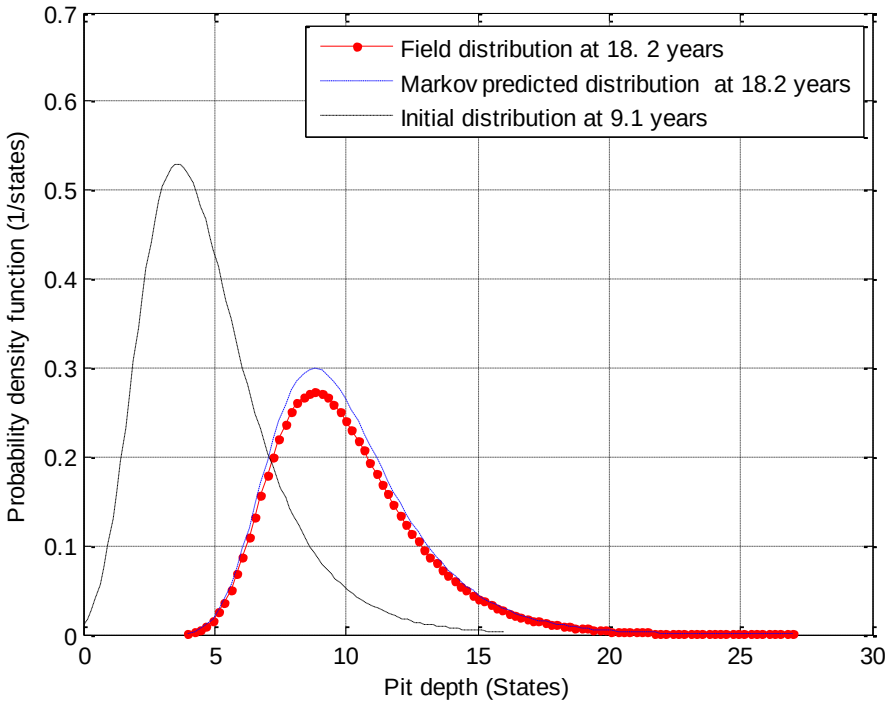

Figure 11b: Comparison of Markov model prediction and field measured pit depths distribution for N-80 grade well tubing at 18.2 years from initial field distribution at 9.1 years

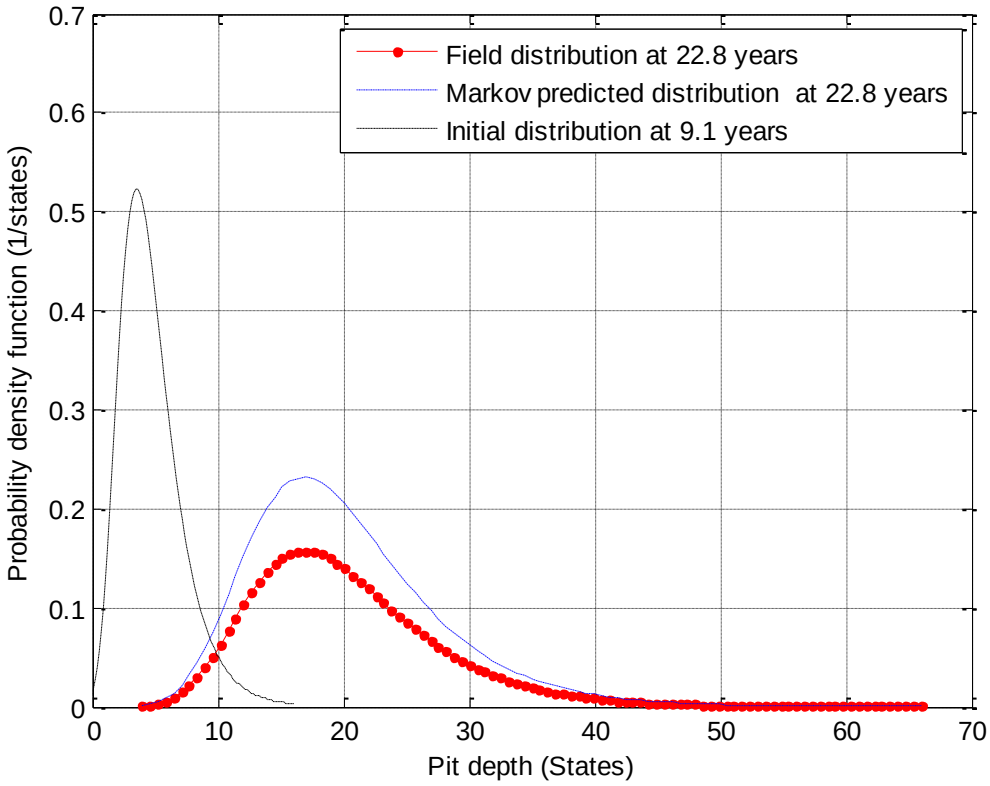

Figure 11c: Comparison of Markov model prediction and field measured pit depths distribution for N-80 grade well tubing at 22.8 years from initial field distribution at 9.1 years

4.1.2 Modelling Pitting Distribution of In-line Inspected transmission pipeline

The prediction model developed in this research was further validated with magnetic flux leakage in-line inspection data of a 3.7 km X52 grade oil transmission pipeline inspected in August 2012. The inspection on this 203 mm external diameter and 8.7 mm thick pipeline commissioned in 1994 was carried out according to ASME BG31G standards [43]. A total of 1037 pit depths that ranged from 10% to 60% of the pipeline wall thickness were observed. The pipeline wall thickness was divided into 100 states of 0.087 mm-thick each and the transition probability distribution of the pit depth in 2012 was used as the initial distribution for predicting the future pit depth distribution, hence t_0=18 years, for the pit depth distribution in 2022, Δt=10, t_{int}=3.6 years since the distribution was assumed to fall into all data pitting category as explained previously. To determine the future distribution of the pit depth in 2022, a Monte Carlo simulation framework shown in Figure 12 was utilized to predict the pit depth growth.

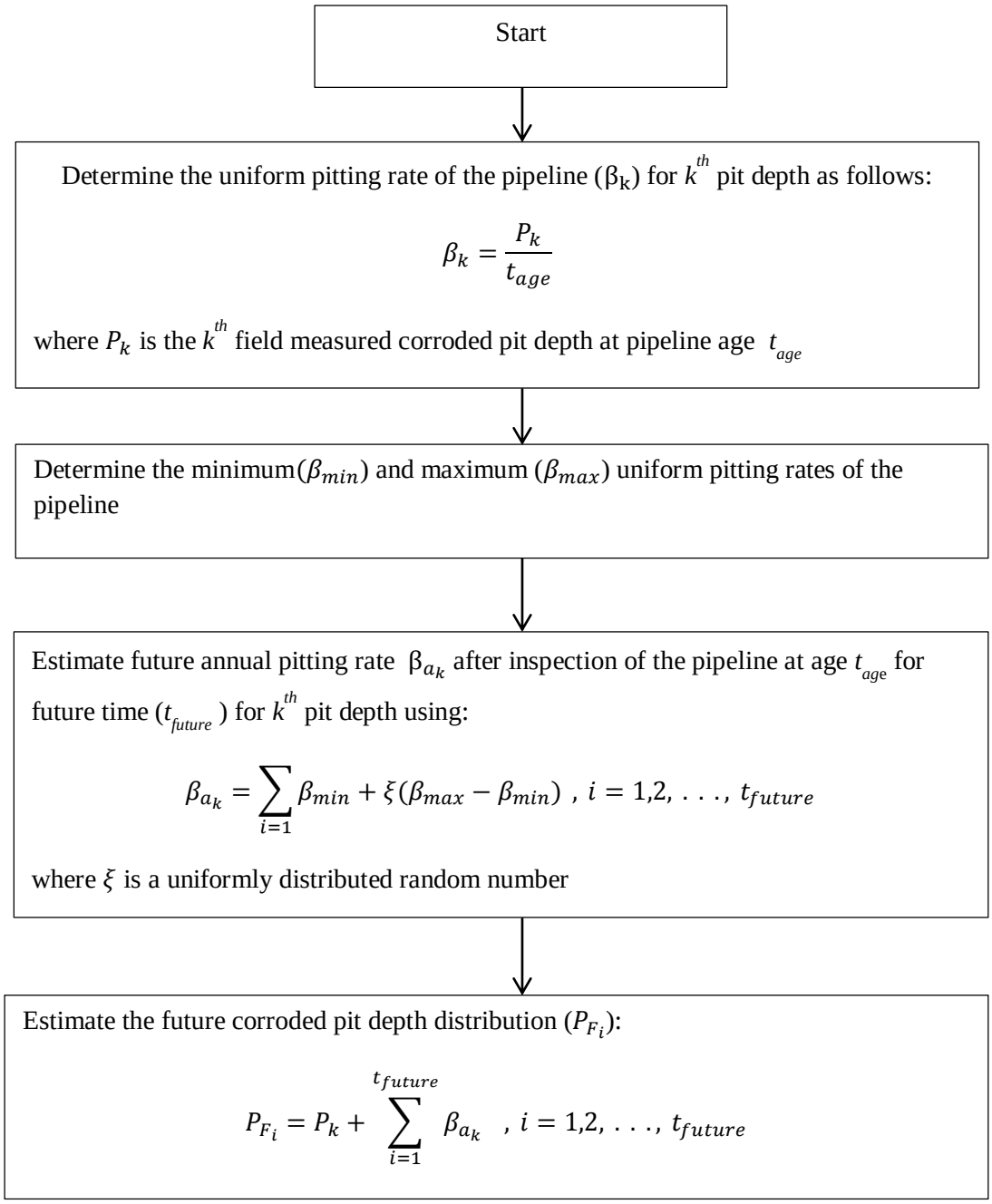

Figure 12: Monte Carlo simulation framework for estimation of future corroded pit depth distribution of a single in-line inspection

Figure 13 shows the pit depths distribution for the field measured in-line inspection data of the pipeline in 2012, Markov predicted and Monte Carlo simulated pit depth distribution in 2022. The goodness of fit test with two-sample K-S test showed that a p-value of 0.6828 made it possible to accept the hypothesis that Markov predicted pit depth distribution came from similar distribution with Monte Carlo simulated distribution of the transmission pipeline.

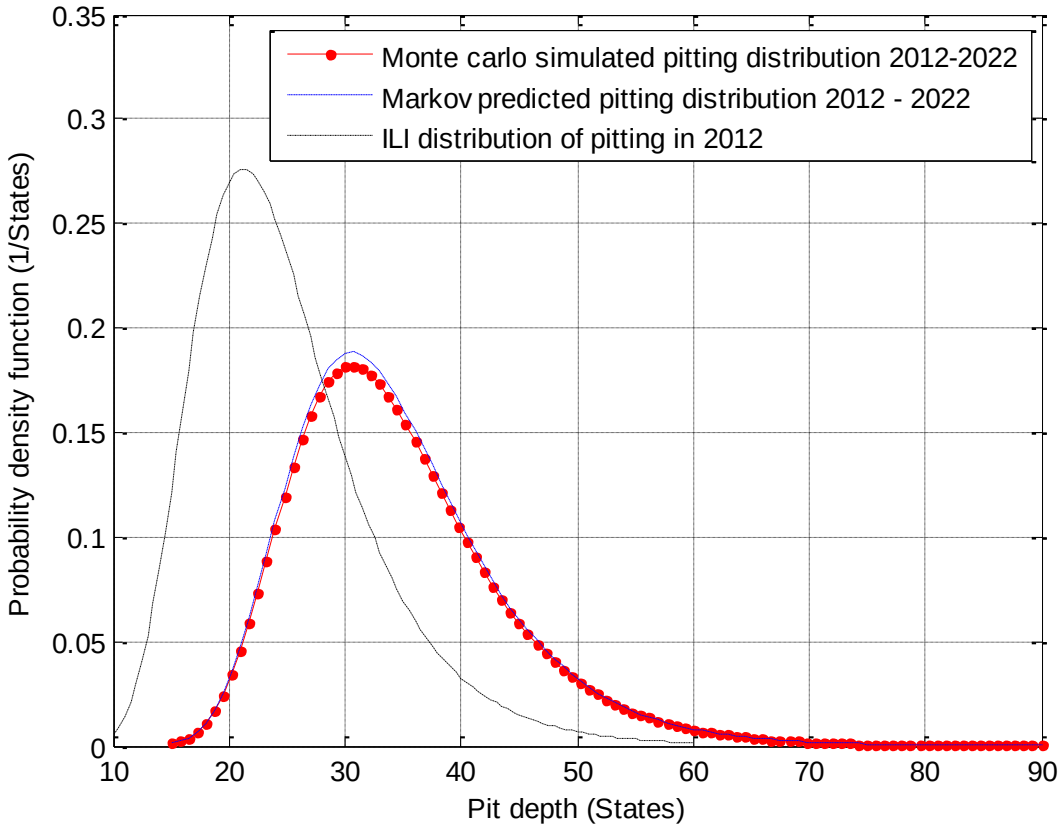

Figure 13: Comparison of Markov predicted and Monte Carlo simulated pit depth distribution in 2022 from initial pitting distribution in 2012

4.2 Validation of the Monte Carlo simulated pit depths

To validate the pit depth data generated by Monte Carlo simulation, the probability density distributions of the field observed data and the Monte Carlo simulated data were compared using the techniques described by other researchers for predicting pit depth growth of pipelines [44-45]. The field observed maximum pit depths were tested with Kolmogorov Smirnov goodness of fit test for different distributions – Generalized Extreme Value (GEV), Weibull and lognormal and lognormal distribution was found to be the best fitting distribution (see Figure 14). Other researchers have also shown that lognormal distribution was the best fit distribution for studied pit depths [26, 42]. The comparison of the lognormal distributions of the field and simulated pit depths is shown in Figure 15. A two-sample Kolmogorov Smirnov goodness of fit test shows that a p-value of 0.995 is enough to accept the hypothesis that both simulated and field observed distributions are similar whereas a root mean square error of 0.0012 indicates that Monte Carlo simulated pit data has not varied much when compared with the field observed data.

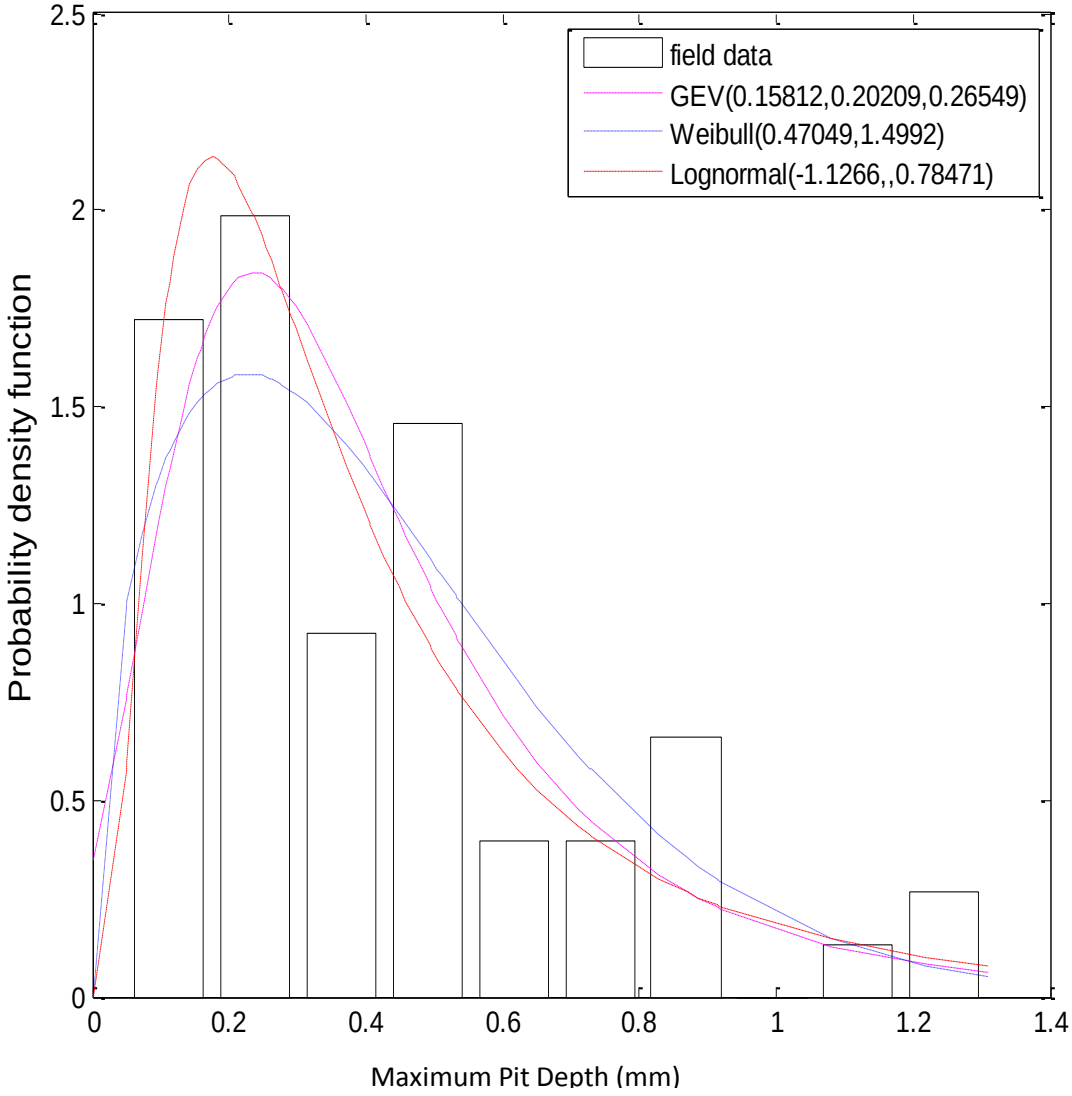

Figure 14: Probability density function distribution of field measured data

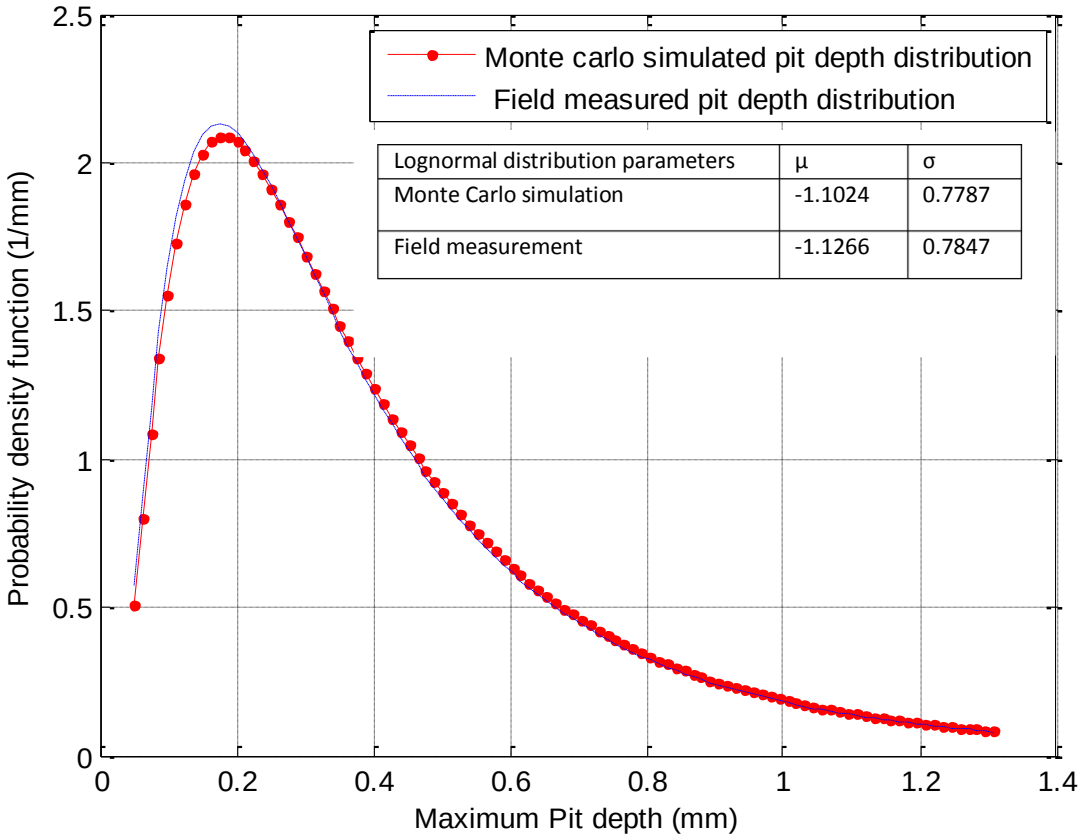

Figure 15: Comparison of pit depth distribution for field and Monte Carlo simulated data

4.3 Validation of the Markov Prediction Model

Root Mean Square Error (RMSE) was also used to validate the field observed pit depth data and Markov predicted data. The summary of the RMSE for the tested field data are shown in Table 3.

Table 3: Summary of the RMSE of the tested field data

L-80 Grade Well Tubing	
Age (years)	RMSE
5.8	0.0368
N-80 Grade Well Tubing	
Age (years)	RMSE
15.3	0.0616
18.2	0.0724
22.2	0.0869
X52 Transmission Pipeline	
Year	RMSE
2022	0.0154

Table 3 indicates that the error in Markov estimation of the future pit depth of the tested field data is between 1.54% and 8.69%. This result implies that Markov model prediction of future pit depth distribution is over 90% accurate.

5.0 Conclusions

To estimate the future pit depth distribution of oil and gas pipelines, a non-homogenous, continuous time pure birth Markov process was used. The work focused on internal pitting corrosion of oil and gas pipelines by considering the effects of some operating parameters – temperature, CO_2 partial pressure, pH and flow rate on the pit depth growth at different pitting categories stipulated by NACE. The pipeline wall thickness was divided into a number of states and the pit depths categorized into the states whilst the transition probability functions estimated by using a closed form of negative binomial distribution was used to estimate the future pit depths distribution.

By analysing the operational parameters and pit depths of the pipelines, the pitting initiation times were estimated for different categories of pitting corrosion rates. The Markov predicted model was tested with field data from L-80 and N-80 grades of well tubing used in offshore oil and gas production and the results agrees well. Onshore oil and gas transmission pipeline inspection data for X52 grade pipe was also tested with the Markov prediction model and the result showed a good agreement with future pit depth distribution modelled with discrete events Monte Carlo simulation.

The field data was also compared with data obtained from the Monte Carlo simulation experiment and the error in the prediction was less than 1%. The comparison of the Markov predicted model and the field data indicated an accuracy of 91.3%~ 98.5%. Since this model has predicted successfully the future pit depth distribution for similar materials in different oil and gas producing wells, it will be a vital tool for pipelines reliability management.

References

1. A. Valor, F. Caleyo, L. Alfonso, J. C. Velazquez, J.M. Hallen, Markov Chain Models for the Stochastic Modeling of Pitting Corrosion, Mathematical Problems in Engineering, vol. 2013, Article ID 108386, 13 pages, 2013.
2. R. E. Melchers, Extreme value statistics and long-term marine pitting corrosion of steel, Probabilistic Engineering Mechanics, 23(4) (2008)482-488.
3. D. Rivas, F. Caleyo, A. Valor, J. M. Hallen, Extreme value analysis applied to pitting corrosion experiments in low carbon steel: Comparison of block maxima and peak over threshold approaches, Corrosion Science 50(2008)3193–3204.
4. S. Papavinasam, A. Doiron, R. W. Revie, Model to Predict Internal Pitting Corrosion of Oil and Gas Pipelines. Corrosion, 66(3) (2010) 035006-035006-11.
5. K. R. Tarantseva, Models and Methods of Forecasting Pitting Corrosion. Protection of metals and physical chemistry of surfaces, 46(1) , (2010)139-147

6. S. Yusof, N. M. Noor, N. Yahaya, A. S. A. Rashid, Markov chain model for predicting pitting corrosion damage in offshore pipeline. Asian Journal of Scientific Research, 7(2) (2014) 208-216.
7. S. Zhang, W. Zhou, H. Qin, Inverse Gaussian process-based corrosion growth model for energy pipelines considering the sizing error in inspection data. Corrosion Science, 73(2013) 309-320.
8. A. Valor, F. Caleyo, D. Rivas, J. M. Hallen, Stochastic approach to pitting-corrosion-extreme modelling in low-carbon steel, Corrosion Science, 52(3) (2010) 910-915.
9. A. K Sheikh, J. K. Boah, D. A. Hansen, Statistical Modeling of Pitting Corrosion and Pipeline Reliability, Corrosion, 46(3) (1990) 190-197.
10. J. C. Velazquez, F. Caleyo, A. Valor, J. M. Hallen, Predictive model for pitting corrosion in buried oil and gas pipelines. Corrosion 65(5) (2009) 332-342.
11. E. Bolanos-Rodriguez, J. C. González Islas, G. Y. Vega-Cano, E. Flores-García, Modeling based on markov chains for the evolution of pitting corrosion in buried pipelines carrying gas. Paper presented at the ECS Transactions, 35(17) (2011)37-42.
12. F. Caleyo, J. C. Velázquez, A. Valor, J. M. Hallen, J. M. Markov chain modelling of pitting corrosion in underground pipelines, Corrosion Science 51(2009)2197–2207.
13. E. S. Rodriguez III, J. W. Provan, Part I: Development of a general failure control system for estimating the reliability of deteriorating structures. Corrosion, 45(3) (1989)178-192.
14. E. N. Camacho, E. Frutuoso , P. F. Melo, P. L. C. Saldanha, E. P. Da Silva, A fokker-planck model of pitting corrosion in underground pipelines to support risk-informed decision making. Paper presented at the Advances in Safety, Reliability and Risk Management - Proceedings of the European Safety and Reliability Conference, ESREL, (2012)2993-2999.
15. R. E. Melchers, Representation of uncertainty in maximum depth of marine corrosion pits. Structural Safety, 27(4) (2005) 322-334.
16. R. E. Melchers, Estimating uncertainty in maximum pit depth from limited observational data. Corrosion Engineering Science and Technology, 45(3) (2010) 240-248.
17. R. E. Melchers, Representation of uncertainty in maximum depth of marine corrosion pits. Structural Safety, 27(4) (2005) 322-334.
18. P. J. Laycock, R. A. Cottis, P. A. Scarf, Extrapolation of Extreme Pit Depths in Space and Time. Journal of Electrochemical Society 137(1) (1990)64-69.
19. F. Caleyo , J.C. Velázquez , A. Valor , J.M. Hallen, Probability distribution of pitting corrosion depth and rate in underground pipelines: A Monte Carlo study. Corrosion Science 51(2009)1925–1934
20. Y. Chen, R. Howdyshell, S. Howdyshell, L. Ju, Characterizing pitting corrosion caused by a long-term starving sulfate-reducing bacterium surviving on carbon steel and effects of surface roughness. Corrosion In-Press, 2014.

21. A. Valor, F. Caleyo, L. Alfonso, D. Rivas, J. M. Hallen, Stochastic modeling of pitting corrosion: A new model for initiation and growth of multiple corrosion pits, Corrosion Science, 49(2)(2007)559-579.
22. G. Engelhardt, D. D. Macdonald, Deterministic Prediction of Pit Depth Distribution. Corrosion, 54(6)(1998)469-479.
23. A. Valor, F. Caleyo, J. M. Hallen, J. C. Velazquez, Reliability assessment of buried pipelines based on different corrosion rate models, Corrosion Science 66 (2013)78-87.
24. J. C. Velazquez, A. Valor, F. Caleyo, V. Venegas, J. H. Espina-Hernandez, J. M. Hallen, M. R. Lopez, Pitting corrosion models improve integrity management, reliability. Oil and Gas Journal, 107(28)(2009) 56-62.
25. S. Zhang, W. Zhou, System reliability of corroding pipelines considering stochastic process-based models for defect growth and internal pressure, International Journal of Pressure Vessels and Piping 111-112 (2013)120-130.
26. F.A.V. Bazán, A. T. Beck, Stochastic process corrosion growth models for pipeline reliability, Corrosion Science 74 (2013) 50–58.
27. A. Valor, F. Caleyo, L. Alfonso, J. Vidal, J. M. Hallen, Statistical Analysis of Pitting Corrosion Field Data and Their Use for Realistic Reliability Estimations in Non-Piggable Pipeline Systems. Corrosion In-Press, 2014.
28. E. S. Rodriguez III, J. W. Provan, Part II: Development of a general failure control system for estimating the reliability of deteriorating structures. Corrosion, 45(3)(1989) 193-206.
29. Y. Katano, K. Miyata, H. Shimizu, T. Isogai, Predictive Model for Pit Growth on Underground Pipes, Corrosion, 59(2) (2003) 155-161.
30. I. S. Cole, D. Marney, The science of pipe corrosion: A review of the literature on the corrosion of ferrous metals in soils, Corrosion Science 56 (2012) 5–16
31. C. C. White III, D. J. White, Markov Decision Process. European Journal of Operational Research 39(1989)1-16.
32. R. M. Feldman, C. Valdezffores, Applied probability and stochastic processes 2nd edition. Springer, New York, 2010, ISBN: 978-3-642-05155-5.
33. E. Parzen, stochastic Processes, Classics in Applied Mathematics, Society for Industrial and Applied Mathematics (SIAM), PA, 1999.
34. H. M. Taylor, S. Karlin, An introduction to stochastic modelling 3rd edition. Academic press San Diego, California USA, 1998, ISBN-13:978-0-12-684887-8.
35. M. Ahammed, R.E. Melchers, Reliability estimation of pressurised pipelines subject to localised corrosion defects, International Journal of Pressure Vessels and Piping, 69(3) (1996) 267-272.

36. S. Li, S. Yu, H. Zeng, J. Li, R. Liang, Predicting corrosion remaining life of underground pipelines with a mechanically-based probabilistic model, Journal of Petroleum Science and Engineering, 65(3-4) (2009) 162-166.
37. F. Caleyo, J.L. González, J.M. Hallen, A study on the reliability assessment methodology for pipelines with active corrosion defects, International Journal of Pressure Vessels and Piping, 79(1) (2002) 77-86.
38. M. Ahammed, Probabilistic estimation of remaining life of a pipeline in the presence of active corrosion defects, International Journal of Pressure Vessels and Piping 75(4) (1998) 321-329.
39. NACE standard RP0775, Preparation, installation, analysis and interpretation of corrosion coupons in oilfield operations. NACE international, Houston, TX. USA, 2005.
40. A. J. McMahon, D. M. E. Paisley, Corrosion Prediction Modelling - A Guide to the Use of Corrosion Prediction Models for Risk Assessment in Oil and Gas Production and Transportation Facilities, Report No. ESR.96.ER.066, BP International, Sunbury, 1997
41. D. Martínez, R. Gonzalez, K. Montemayor, A. Juarez-Hernandez, G. Fajardo, and M. A. L. Hernandez-Rodriguez, Amine Type Inhibitor Effect on Corrosion–Erosion Wear in Oil Gas Pipes, Wear, 267 (2009), 255-58.
42. M. H. Mohd, J. K. Paik, Investigation of the corrosion progress characteristics of offshore subsea oil well tubes, Corrosion Science 67(2013)130-141.
43. ASME, Manual for determining the remaining strength of corroded pipelines. American Society of Mechanical Engineers, B31G, New York, 2009.
44. M. H. Mohd, D. K. Kim, D. W. Kim, J. K. Paik, A time-variant corrosion wastage model for subsea gas pipelines, Ships and offshore structures, 9(12)(2014) 161-176.
45. J. K. Paik, D. K. kim, Advanced method for the development of an empirical model to predict time-dependent corrosion wastage, Corrosion science 63(2012) 51-58.